# Chapter 5. Effects of Vegetation on Stream Bank Erodibility and Critical Shear Stress

The overall goal of this research is to compare the effects of woody and herbaceous vegetation on stream bank erosion. This chapter presents the third of three substudies that address the impact of vegetation on stream bank erosion. The goal of this study was to determine the erodibility of rooted stream bank soils and to evaluate the relative effects of vegetation type, root density, and freeze-thaw cycling on the erodibility of stream banks

## 5.1. Methods

### *5.1.1. Jet Testing*

To evaluate the effects of vegetation on stream bank soil erodibility and critical shear stress, the upper and lower banks at each site were tested in situ using a multiangle submerged jet test device (ASTM, 1999a; Hanson and Cook, 1997). The jet test device is shown in Figure 5.1 and Figures G1-G5 in Appendix G. The device consisted of a 30.5 cm diameter steel base ring that was pounded into the soil to a depth of 7.6 cm to prevent piping of water under the ring (Figure G2). The tank top, which consisted of two concentric plexiglass tubes centered perpendicular to a clear circular plexiglass sheet was then latched onto the base ring (Figure G1). The upper third of the tank top was hinged so the tank lid could be opened during the test without taking the top off the base ring (Figure 5.1). The outer plexiglass tube had a 6.35 mm diameter circular orifice that served as the jet nozzle. The inner tube served to stabilize the point gage, which was inserted into the plexiglass tubes and lowered through the nozzle. Before the start of each test, the point gage was used to measure the distance to the nozzle opening and the initial soil surface. Water was pumped from the stream to a plexiglass head tank (Figure G3) and then to the outer plexiglass tube. The head tank was used to control the hydraulic shear stress and to dampen fluctuations in pumping level. The deflecting plate was placed in front of the nozzle and the base ring was filled with water. Once the base tank was filled, the deflector plate was removed to start the test.

The distance to the soil surface (scour depth) and the pressure drop across the nozzle were measured at regular intervals throughout the test. The point gage tip was the same diameter as the nozzle, so the jet was stopped each time a scour measurement was made. Where possible,

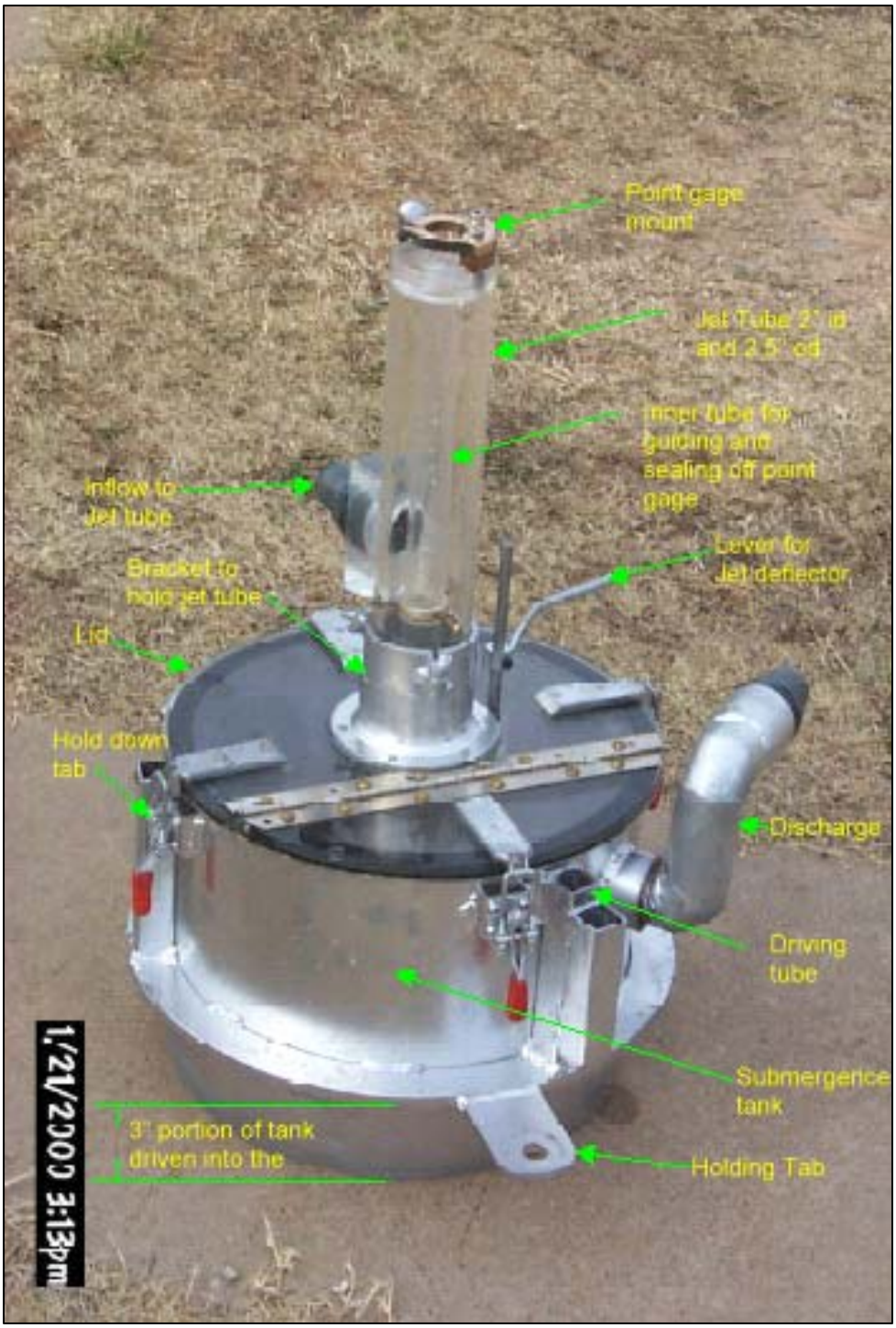


Figure 5.1. Multiangle submerged jet testing device (picture courtesy of Dr. Greg Hanson, Research Hydraulic Engineer, USDA-ARS Hydraulics Engineering Research Unit, Stillwater, OK).

three test runs were conducted at each site; each test was run at a different head setting and location to provide an average soil erodibility per site over a range of hydraulic stresses. While the tests should ideally be run within the range of shear stresses expected in each stream, from a practical standpoint, they were conducted at shear stresses great enough to cause erosion of the bank material, but not great enough to undermine the base ring. Each run was conducted at a different head setting, with the head settings varying from 20 – 30 cm (approximately 20 - 40 Pa) between runs. Results from the three jet tests were averaged to produce a single soil erodibility ($K_d$) and critical shear stress ($\tau_c$) for each site.

Test durations generally range from 30 to 60 minutes with measurement intervals of 5 or 10 minutes. To determine the optimal test duration and measurement interval, three 90 minute tests were conducted with 5 minute measurement intervals. Both $K_d$ and $\tau_c$ were calculated for a 45 minute test duration with measurements at 5 minute intervals and for a 90 minute test run with scour measurements at 10 minute intervals. Results from these tests indicated that the erodibility coefficient decreased from 24 - 49% by increasing test time from 45 to 90 minutes. This reduction is likely due to the weathering of the surface soil layers by subaerial processes. The erosion rate is often rapid initially and then reduces to a constant or near zero level after 20 to 30 minutes, depending on the soil type, as more resistant material is encountered with increasing scour depth. Results for $\tau_c$ were inconclusive: doubling the test duration and measurement interval created changes in $\tau_c$ from -87% to +662%. Because the Blaisdell model (Blaisdell et al., 1981) appeared to fit the data better with a shorter test duration and more frequent measurement interval and because the erosion rate frequently leveled off after 20 minutes, a 45 minute test duration with 5 minute measurement intervals was chosen for the experiments.

The soil erodibility coefficient was determined for two depths on each bank, coinciding with the placement of the temperature sensors (Chapter 4). The exception to this was site ST2, where the bank height was not sufficient for two tests, so tests were run for the upper bank only. The location along the stream for each run was chosen using a stratified random technique, where possible (Ott, 1993). Large woody vegetation, large roots, and animal burrows (particularly crawfish) frequently precluded testing at certain locations. Figure 5.2 shows one test run setup at site TC4, which had a dense riparian forest. On the upper banks of sites EL1

Figure 5.2. Jet test setup at heavily wooded site, TC4.

and TC7, as well as the lower bank of TC6, only two jet tests were performed due to problems with tank undermining during testing. No testing was possible on the upper bank of site TC6 due to the presence of an extensive network of crawfish burrows.

This study represents the first application of submerged jet testing to vegetated stream banks; thus, some adjustments to the testing procedure were made. Each site was prepared to provide a relatively uniform initial test surface for each run. Following selection of a test location, all the vegetation on the testing site was clipped to ground level in an approximately 45 cm diameter circle. Large irregularities in the soil surface were gently removed with scissors or a small shovel. At sites where the upper bank was cantilevered, the cantilevered soil was gently removed with a shovel and any exposed roots were cut to the ground level (Figure 5.3). Prior to setting the base ring, it was placed on the soil to mark the ring diameter. The soil along this circle was then probed with a small keyhole saw to cut any large roots and to locate any animal burrows or large holes. Following this investigation, the tank was pounded into the soil using a

Figure 5.3. Prepared bank surface prior to jet testing.

slide hammer and the soil on the outside of the tank was compacted with a large hammer. The soil at the inside edge of the tank was also gently compacted by hand and sealed using bentonite to prevent undermining of the jet test tank (Figure 5.4). Because filling of the tank through the nozzle frequently resulted in undermining of the test tank, the tank was initially filled using small syphon hose and a large plastic bottle.

### *5.1.2. Soil and Water Characteristics*

Soil samples were taken for each jet test run to evaluate root density and soil parameters shown to affect soil erosion in previous studies (Table 5.1). Because root density varies greatly over small spatial scales, a single soil core (7 cm diameter, 15-cm long) was taken in the jet test tank following testing to measure root density at the test site. The soil samples were frozen in a chest freezer until analysis. To determine root density, the soil cores were thawed in a bucket of

Figure 5.4. Bentonite seal around tank edge following test run.

Table 5.1. Soil tests conducted and methodology used.

| **Parameter** | **Method** |
|---|---|
| Grain size distribution (percent clay, silt, sand, and gravel; median diameter, $D_{50}$; standard deviation, $\sigma$) | USDA, 1996 |
| Soil specific gravity ($\gamma$) | ASTM D854-92 (ASTM, 1999c) |
| Bulk density | USDA, 1996 |
| Moisture content | USDA, 1996 |
| Atterberg limits | ASTM D4318-98 (ASTM, 1999b) |
| Aggregate stability | USDA, 1996 |
| Organic carbon | Walkley and Black, 1934; Jackson, 1958; Allison, 1965 |
| pH | USDA, 1996 |
| Specific electrical conductivity | USDA, 1996 |
| Major soil cations ($Ca^{2+}$, $Mg^{2+}$, $K^{+}$, $Na^{+}$) | USDA, 1996 |

water and washed over a No. 35 sieve (0.5 mm mesh). The soil and roots retained on the sieve were then placed in a white plastic pan and the live roots were removed by hand and stored in a refrigerator at 4$^{o}$C until scanning. Root length and root volume were measured for each of the five diameter classes (< 0.5 mm, 0.5-2.0 mm, 2-5 mm, 5-10 mm and 10-20 mm) using a Régent Instruments STD 1600+ scanner and WinRHIZO$_{TM}$ analysis software (Arsenault et al., 1995; Régent Instruments Inc, Quebec, Canada).

Because cohesive soils are eroded as aggregates, aggregate stability has a profound influence on soil erodibility. Intact soil blocks roughly 5 x 5 x 10 cm in size were gently removed from the bank face near each jet test location using a small shovel. Samples were air-dried in the laboratory and analyzed within two weeks of sampling. The aggregate stability of 1-2 mm air-dry aggregates was tested using Five Star Scientific (Twin Falls, ID) wet sieving apparatus, according to procedures outlined by the USDA Soil Center (USDA, 1996).

Soil organic carbon content was also tested due to its influence on aggregate stability and because some researchers have suggested that plant exudates may play a role in the stability of stream bank soils (Brady, 1984; Amarasinghe, 1992; Thorne et al., 1997). As with aggregate stability, soil samples were taken near the jet test location and air dried until analysis. The Walkley-Black method was used to determine the soil organic carbon content (Walkley and Black, 1934; Jackson, 1958; Allison, 1965).

Soil physical properties, such as the Atterberg Limits, specific gravity, bulk density, and antecedent moisture content, also influence the erosion of cohesive soils (Grissinger, 1982). Soil Atterberg limits are the liquid limit, the plastic limit, and the plasticity index. The liquid limit is the lowest moisture content at which viscous flow will occur, while the plastic limit is the lowest moisture content at which a 1/8 inch soil thread will remain intact during rolling. The difference between these two parameters is the plasticity index, which defines the range of moisture contents over which a soil is plastic. It is dependent on the amount and type of clay and is a useful indicator of the character of fine grained soils (Lambe and Whitman, 1969; Holtz and Kovacs, 1981). Another parameter, the activity of a clay, is defined as the plasticity index divided by the percent clay content. This parameter is correlated to the type of clay mineral present in the soil (Table 5.2) and is a good comparative index for rating erosion resistance (Paaswell, 1973; McBride, 1994). The clay type affects chemical interactions with the eroding

fluid: high activity indicates high shrink/swell potential (Holz and Kovacs, 1981; McBride, 1994). Soil Atterberg limits were evaluated for air-dry samples according to ASTM standard D4318-98 (ASTM, 1999b).

Specific gravity is the ratio of the mass of a unit volume of soil to the mass of an equivalent volume of deionized water. Soil particles with high specific gravity settle quickly and are less likely to be entrained. The specific gravity of the bank soils was evaluated for air-dry samples according to ASTM standard D854-98 (ASTM, 1999d).

Research has shown soil shear strength increases with increasing bulk density (Asare et al., 1997). The soil antecedent moisture content has varied impacts on soil erosion: increased soil moisture content reduces erosion due to slaking, but increases fluvial entrainment (Craig, 1992; Le Bissonnais, 1996). Soil bulk density and antecedent moisture content were measured by taking a single undisturbed soil core in 5 x 5 cm aluminum cylinder with a slide hammer near each jet test location. Samples were taken prior to each jet test and wrapped in plastic to prevent moisture loss. These samples were weighed and dried at 105$^{o}$C within 8 hours of sampling, following procedures outlined by the USDA soil manual (USDA, 1996).

The remaining soil parameters, pH, potassium intensity factor (KIF), sodium adsorption ratio (SAR), specific electrical conductivity (EC), and the pore water salt concentration (TS and PW), were measured to determine the effect of pore water chemistry on soil erosion. The KIF and SAR are defined as follows:

$$KIF = \frac{\left[K^{+}\right]}{\sqrt{\left(\left[Ca^{2+}\right]+\left[Mg^{2+}\right]\right)}} \tag{5.1}$$

$$SAR = \frac{\left[Na^{+}\right]}{\sqrt{\left(\frac{\left[Ca^{2+}\right]+\left[Mg^{2+}\right]}{2}\right)}} \tag{5.2}$$

where $[K^{+}]$, $[Ca^{2+}]$, $[Mg^{2+}]$ and $[Na^{+}]$ are the concentrations of potassium, calcium, and magnesium, and sodium respectively, in the soil pore water. The KIF is an indication of the

activity of potassium in the soil solution (Brady, 1984). Potassium is one of the major soil cations and is derived primarily from the weathering of micas. The SAR indicates the level of exchangeable sodium in the soil, in relation to calcium and magnesium, and is frequently used in irrigation (Brady, 1984). Soils high in exchangeable sodium are more likely to experience swelling, surface crusting, sealing, erosion, and colloidal dispersion. Additionally, high values of the SAR are indicative of low aggregate stability (McBride, 1984).

Table 5.2. Activities of various minerals.

| Mineral | Activity |
|---|---|
| Na-montmorillonite | 4-7 |
| Ca-montmorillonite | 1.5 |
| Illite | 0.5-1.3 |
| Kaolinite | 0.3-0.5 |
| Allophane | 0.2 |
| Calcite | 0.2 |
| Quartz | 0 |

The pore water salt concentration is indicative of the ionic strength of the pore water, which also influences the dispersivity of clays. Arulanandan et al. (1980) quantified this parameter as the sum of the calcium, sodium, magnesium, and potassium. In general, soil colloids tend to disperse as the salt concentration, cation valence, and temperature of the eroding and soil pore waters decrease. Also, increases in anion adsorption and the dielectric constant, cation size, and pH of the eroding and pore fluids increase clay dispersion (Holtz and Kovacs, 1981).

Soil samples for chemistry analysis were taken near each jet test location using a small shovel and air dried prior to analysis. The three soil samples taken for the upper or lower bank at each site were composited into a single sample. Using approximately 1 kg of well mixed, air dry soil, a saturated paste was created following procedures outlined in the USDA soil manual (USDA, 1996). The pH of the saturated paste was measured with a Corning 360i solid state ion selective field effect transistor electrode. Approximately 30 ml of soil extract was filtered from the saturated paste using a vacuum apparatus with a Whatman No. 40 paper filter (8 μm). For fine grained soils where pore water extraction was excessively slow, a No. 1 filter (11 μm) was

used and the extract was subsequently refiltered with a No. 40 filter. The specific EC of the pore water extract was measured using an Oakton EC Tester Low (0-1999 μs/cm, ±10 μs/cm), while the salt concentrations (sodium, potassium, calcium, and magnesium) were measured by inductively coupled plasma spectrometry at the Virginia Tech Soil Testing Laboratory.

Because the chemistry of the eroding fluid may also influence soil erodibility, the EC, pH, total suspended solids concentration, and temperature of the stream water were tested daily at each site. Electrical conductivity was measured using a Corning CD-30 conductivity meter (0 - 1999 μs/cm, ±1 μs/cm), while a Hach Pocket Pal pH Tester (0 - 14, ±0.1) was used to measure stream pH. Due to the generally low suspended solids content of the streams, a grab sample of approximately one liter of stream water was taken and analyzed for total suspended solids using a 0.45 μm filter according to EPA Method 160.2 (USEPA, 1983). Samples were generally collected at baseflow, although some samples may have consisted partly of stormwater runoff from prior storm events. Stream temperature was measured with a Fisher Scientific Traceable thermometer (-50 $^{o}$C - 300$^{o}$C, ±0.1 $^{o}$C).

*5.1.3. Data Analysis*

Data from the jet tests were evaluated to determine $K_d$ and $\tau_c$, following the procedures of Hanson and Cook (1997). These analytical procedures have been coded in an Excel spreadsheet by Hanson and Cook (1997). The author modified the spreadsheets to accept data input in SI units.

Soil erodibility, critical shear stress, bulk density, aggregate stability, specific gravity, initial soil moisture content, organic carbon content, and Atterberg Limits, as well as RLD and RVR data, for each test run were averaged to provide a single parameter value for the upper or lower bank at each site. The small, medium and large root densities were combined to create the parameters “big root length density” (BRLD) and “big root volume ratio” (BRVR). These parameters consist of the sum of the RLD or RVR for the small, median, and large roots (diameters 5 - 20 mm). Since previous research has shown the sum and the ratio of the soil silt and clay contents are significant (SC and S:C, respectively), these two variables were added to the analysis. Also, differences in water chemistry between the eroding and pore fluids were represented by ratios of soil:water pH and specific EC (SWpH and SWEC, respectively). When the soils for two of the three runs were nonplastic, the average was considered nonplastic. The

liquid limit is the lowest moisture content at which viscous flow will occur, while the plastic limit is the lowest moisture content at which a 1/8 inch soil thread will remain intact during rolling. The difference between these two parameters is the plasticity index, which defines the range of moisture contents over which a soil is plastic. If two of the three samples were plastic, those values were averaged to generate average site Atterberg Limits.

Because environmental data are often skewed, histograms were developed for each parameter and then the data were transformed to improve distribution symmetry (Helsel and Hirsch, 1992). The transformation used for each parameter is listed in Table H5. Following transformation, each variable was normalized by subtracting the sample mean and dividing by the sample standard deviation. By normalizing each independent variable, their relative contribution to the dependent variable can be compared.

The data were analyzed as a single group and then separated into three groups based on physical and chemical soil properties (Elliot et al., 1990). This approach follows the general method used by Allen et al. (1997) to determine the relationship between soil physical properties and the jet test index using regression analysis for 30 streams in Texas (ASTM, 1999a). Utilizing the entire data set, they found poor correlation between the jet index and the soil properties ($r^2 < 0.12$). The correlation improved greatly when the data were split into groups based on clay content and activity.

Following the example of Allen et al. (1997), the study soils were divided into three soil classes. Initially, the soils were separated into plastic (n = 33) and nonplastic soils (n = 15). Because this study had extensive soil chemical and physical data for each observation, K-means cluster analysis was used to further split the plastic soils into two groups (Johnson and Wichern, 1992). Multiple data sets of physical and chemical soil properties were developed for the cluster analyses, including Atterberg limits, bulk density, aggregate stability, specific gravity, organic carbon content, particle size analysis, median grain diameter and standard deviation, soil pH, soil EC, and sodium, potassium, calcium and magnesium contents. Multiple cluster analyses were conducted, each using a different set of soil parameters, to separate the sites into soil groups. Combining the results of the separate cluster analyses, an average group classification number was calculated for each site: sites with a group number less than 1.5 were assigned to Group 1 (n = 18) and the remainder were assigned to Group 2 (n = 15). The nonplastic soils were labeled

Group 3. Statistically significant differences between the soil physical and chemical characteristics of the groups were evaluated using the nonparametric Mann-Whitney test (Neave and Worthington, 1988).

The following exploratory data analysis procedure was conducted on all four data sets (main data set and three subsets). As a first step, the normalized transformed dependent variables, $K_d$ and $\tau_c$, were plotted versus each normalized transformed parameter to determine if a linear or nonlinear relationship between the variables was evident. Theil-Sen nonparametric linear regression was then performed for both $K_d$ and $\tau_c$ to evaluate the individual relationship between each independent variable and the dependent variables (Theil, 1950; Sen, 1968; Hollander and Wolfe, 1973). Theil-Sen regression is not as sensitive to outliers as standard least squares regression and can be a more robust procedure for environmental data. Lastly, to examine the variables for collinearity, Pearson's correlation coefficient was calculated for each pairwise combination of dependent and independent variables.

Following the exploratory analyses, stepwise multiple linear regression was conducted to evaluate which soil, climate, and vegetation parameters had the greatest influence on stream bank soil erodibility and critical shear stress and to generate predictive equations (Kamyab, 1991). Where data were missing (Atterberg limits, freezing data, and water temperature), two regressions were run, one with the parameters removed and one with the sites with missing values removed. The residuals of each significant regression relationship were visually assessed for independence and normality. Multicolinearity was evaluated using variance inflation factors (VIF; Montgomery and Peck, 1982) and regression lack of fit was examined by data subsetting in Minitab (Burn and Ryan, 1983).

## 5.2. Results

A total of 142 jet test runs were conducted from May through August 2003, at $\tau_o$ of 42 – 273 Pa. While these shear stresses were generally greater than the average boundary shear stresses experienced in the stream channels at bankfull discharge, very high stresses were required to cause soil scour at some of the sites (stream boundary shear stresses calculated in Section 5.3.5). The resulting soil erodibility, critical shear stress, aggregate stability, bulk density, antecedent moisture content, organic carbon content, Atterberg limits and root densities

for each run are listed in Tables H1-H2. The averaged or composited values for upper or lower bank are listed in Tables C1, D1, D2, F1, and H3-H4 and include data on soil texture and the major soil cations, $Ca^{2+}$, $Mg^{2+}$, $K^{+}$, and $Na^{+}$. Because soil texture is relatively invariant over time, soil textural data obtained during the root study (Chapter 3) were used. Using composited soil samples taken 30 cm from the bank face for soil textural analysis at each site likely produced some error in the data because in places the stream bank had a coating of deposited soil, ranging in depth from one to two centimeters, that was not the same material as the remainder of the stream bank. This deposited material was generally coarser and more erodible than the original bank soil and likely resulted in an overestimation of $K_d$ and an underestimation of $\tau_c$.

The jet test values for test 1 on the upper bank of EL3 were not included in the analysis (Table H1). During this particular test, an unusually large scour hole was created that actually exceeded the range of the point gage. The author suspects a rodent burrow in the stream bank may have been encountered and so this particular test was dropped from the analysis.

Nine of the individual jet tests were not run for the full 45 minute test duration due to undermining of the base ring during the test. The effect of shortened test time on the jet test results was investigated using the 133 tests with full 45 minute test durations. For each of these tests, $K_d$ and $\tau_c$ were recalculated using the data from the first 25 minutes of the tests. Theil-Sen regression analyses were then conducted with these data to predict the erosion parameters using the shortened test data. Decreasing the test duration resulted in median increases in $K_d$ and $\tau_c$ of 41% and 2%, respectively. Highly significant regressions were developed for both $K_d$ and $\tau_c$ to predict these parameters for a full test duration, given parameters from a 25 minute duration test. These equations are plotted in Figures 5.5 and 5.6 with the data. The regression equations were then used to adjust the erosion parameters for the nine abbreviated tests.

Typical scour plots for three individual tests are shown in Figure 5.7. Erosion was usually rapid initially and then decreased asymptotically (Stein et al., 1993). The initially high erosion rate may have been the result of weathering of the bank surface. Additionally, as the scour hole deepened, the applied shear stress dissipated, thus reducing erosion (Laursen, 1952). While the test was run immediately following filling of the tank, the slow, gentle filling of the tank with a syphon likely reduced erosion due to slaking; air bubbles from the soil were frequently observed while filling the tank. For tests where erosion occurred as large aggregates

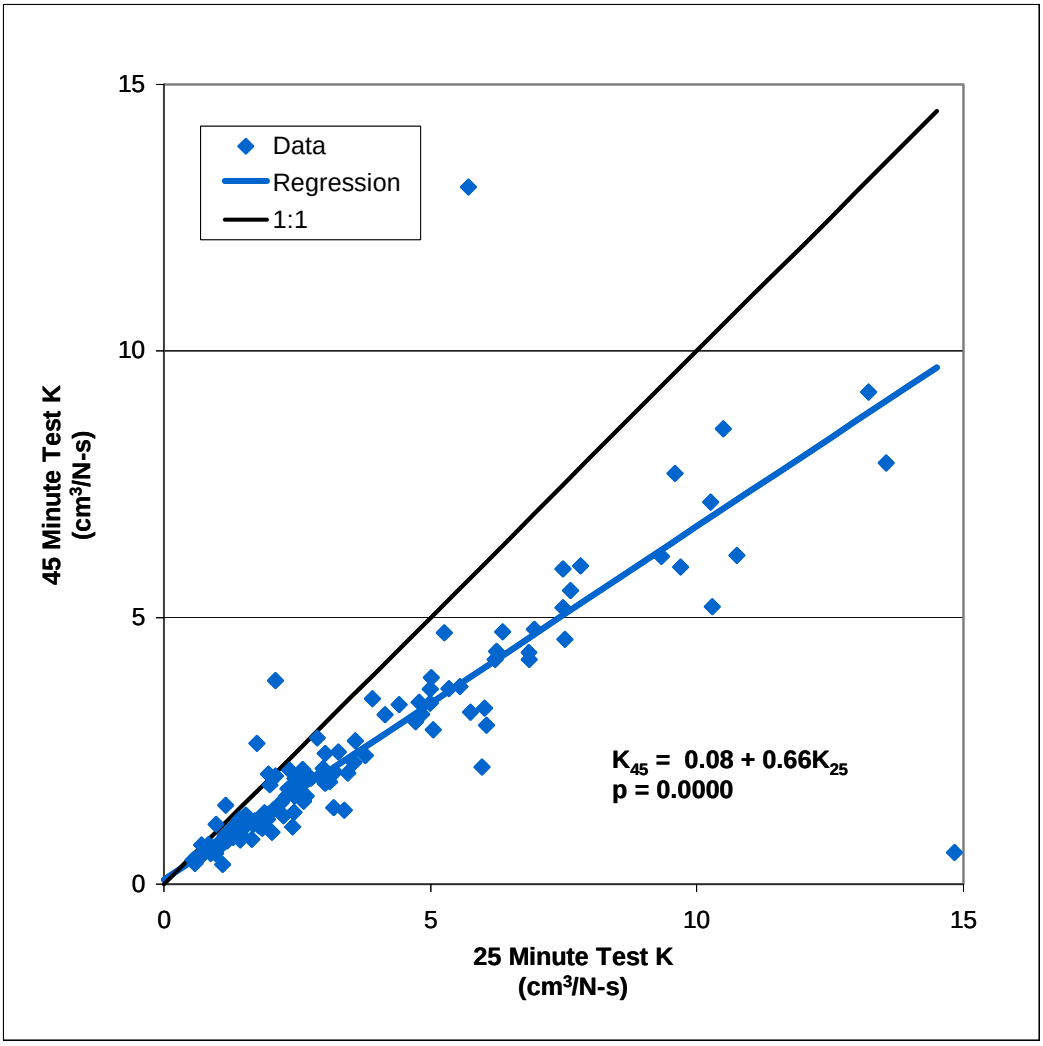


Figure 5.5. The effect of test duration on the soil erodibility coefficient.

(Figure 5.8), the erosion rate varied greatly throughout the test, at times approaching zero and then suddenly increasing. Similar observations have been made in other laboratory and field studies of cohesive soils (Moore and Masch, 1963; Grissinger et al., 1981).

Stream bank erodibility for individual jet test runs ranged from 0.177 $cm^3$/N-s for the moderately resistant lower banks of site ST3 to a maximum of 13.1 $cm^3$/N-s for the lower bank of site SR3, where the soils were highly mobile and dominated by fine sands (Table 5.3). The critical shear stresses varied from 0 Pa to 21.9 Pa. At an individual site, erodibility and critical shear stress varied by as much as one and four orders of magnitude, respectively. This wide

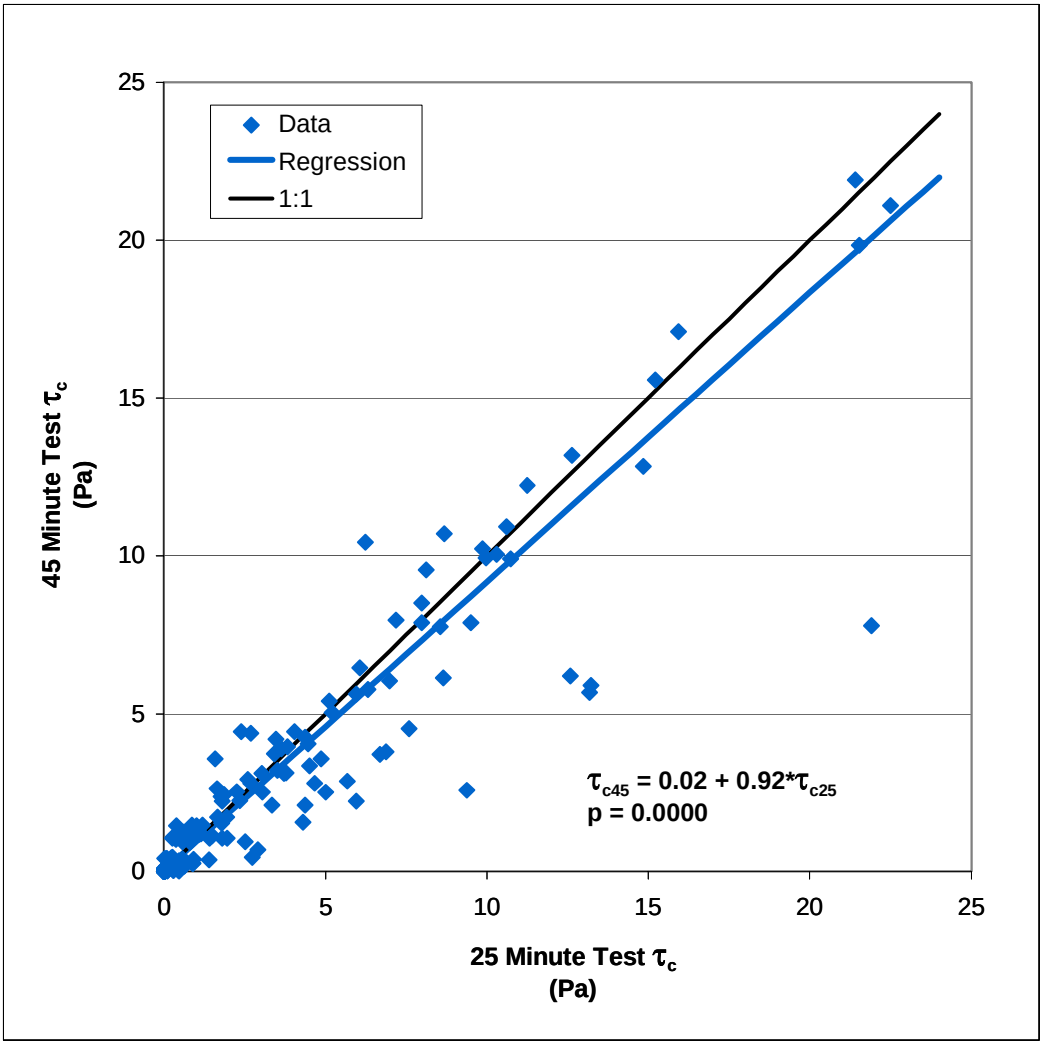


Figure 5.6. The effect of test duration on the soil critical shear stress.

range in data has been observed by other researchers (Grissinger et al., 1981; Hanson and Simon, 2001). Hanson and Simon (2001) noted variation in average site $K_d$ by four orders of magnitude and variation in $\tau_c$ of six orders of magnitude. They attributed this variability within individual stream systems to differences in subaerial exposure, weathering, and cracking along planes of weakness.

As shown in Figure 5.9, there is an inverse exponential relationship between $K_d$ and $\tau_c$. Using nonparametric Theil-Sen regression, a highly significant (p=0.0003) equation was fit to the data, $K_d = 3.1\tau_c^{-0.37}$. A similar equation was determined using simple least-squares regression

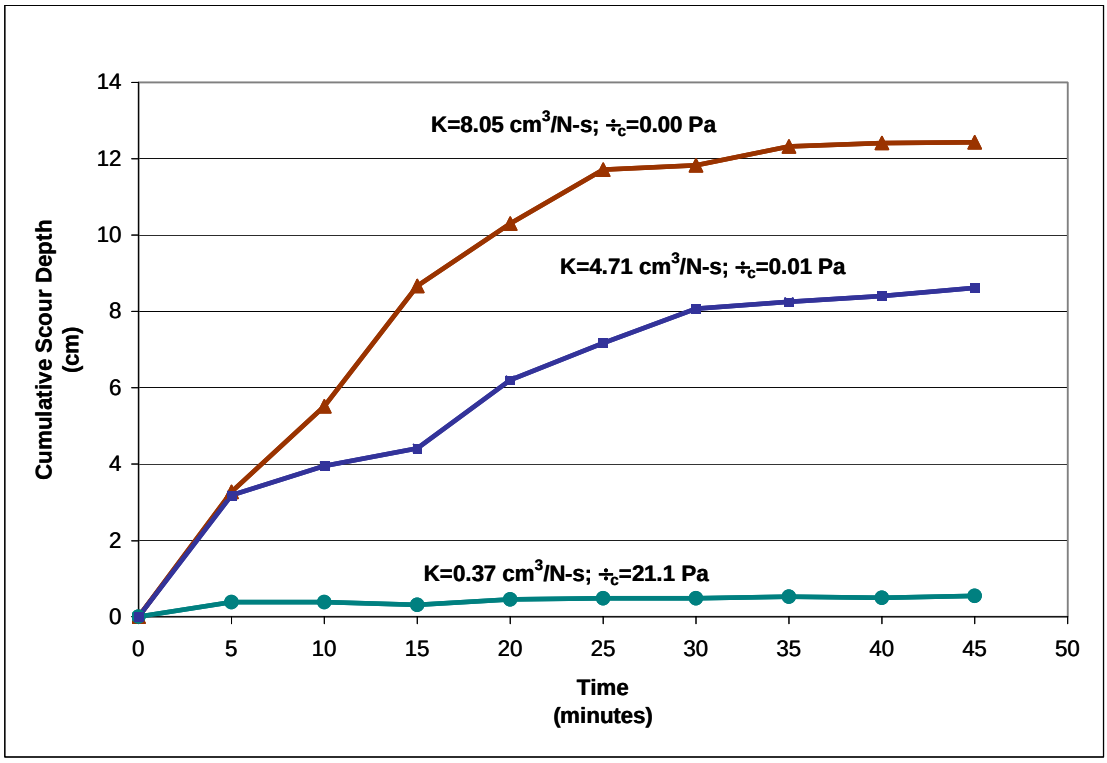

Figure 5.7. Typical scour plots from jet testing.

($K_d = 2.7\tau_c^{-0.28}$; p = 0.0000, $r^2 = 0.263$). Similar results were reported by Arulanandan et al. (1980) and Hanson and Simon (2001). Hanson and Simon fit an exponential equation to data from stream beds in the loess area of the Midwestern US, although the coefficient was not as large (0.2) and the exponent was greater in magnitude (-0.5). The correlation coefficient was much higher for their data ($r^2 = 0.64$), indicating that other parameters may be influencing the erosion rates measured in this study. In two studies of the effects of live roots on rill erosion, Mamo and Bubenzer (2001a,b) found no significant relationship between $\tau_c$ and $K_d$. The authors suggested that soil $\tau_c$ is more a function of the initial soil surface conditions, while $K_d$ depends more on the bulk soil properties. These studies were conducted on disturbed soils and the authors indicated the surface soil was loose and easily eroded. For natural, undisturbed soils, $\tau_c$ may be better correlated to $K_d$.

Hanson and Simon (2001) evaluated $K_d$ and $\tau_c$ for stream beds in the loess area of the Midwestern US, classifying the bed material from very resistant to very erodible. Figure 5.10

Figure 5.8. Eroded aggregates at bottom of jet test tank.

shows the average jet test results for the stream banks in this study plotted by watershed on the scale used by Hanson and Simon. While there is some general grouping of the data by stream system, considerable variability exists and overlap of the data across streams occurs. The results indicate that the stream banks in this study are generally erodible or very erodible. This would be expected from the overall low clay content of the soils and the fact that the tests were carried out on the stream banks and not the stream beds. It is likely stream banks would be more erodible than the stream beds since the stream bank soils are typically finer grained than the stream bed materials.

The effect of $\tau_o$ on $K_d$ and $\tau_c$ was investigated using regression analysis. The three parameters were transformed and normalized, as described in Section 5.1.3, and least-squares regression analysis was conducted to determine the influence of $\tau_o$ on $K_d$ and $\tau_c$. Results of this analysis show that both $K_d$ and $\tau_c$ were significantly influenced by $\tau_o$, but the influence was limited. Soil erodibility was inversely related to the test shear stress ($K_{dNT} = -0.41\tau_{oNT}$;

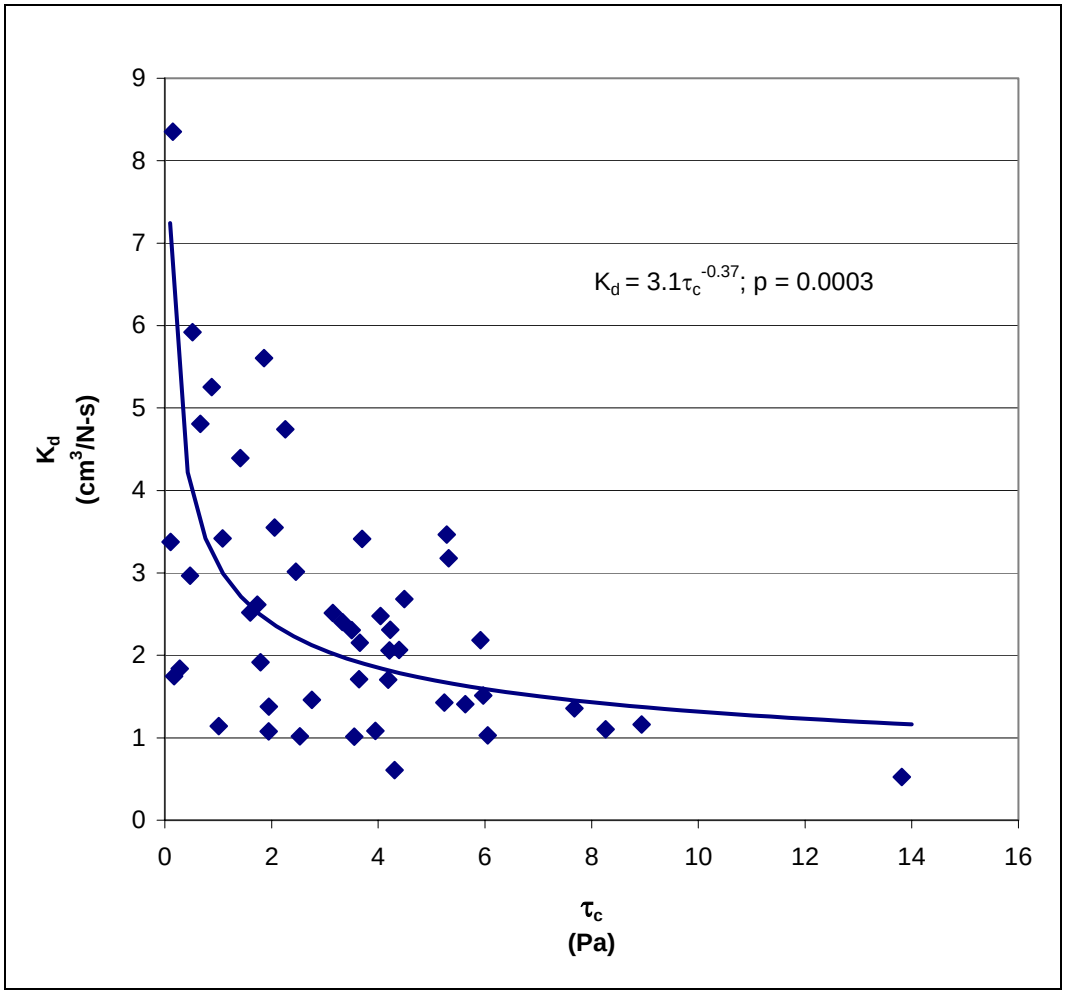


Figure 5.9. Relationship between average stream bank soil erodibility and critical shear stress.

p = 0.000), but $\tau_o$ explained only 16.4% of the variance in $K_d$. The subscript "NT" is used to indicate those variables that have been transformed (Table H6) and normalized. Similarly, $\tau_o$ explained only 7.7% of the variance in $\tau_c$ ($\tau_{oNT} = 0.28\ \tau_{oNT}$; p = 0.001). As indicated by the regression coefficient, the critical shear stress increased with increasing $\tau_o$. Based on these analyses, it appears that running the jet test at higher shear stresses than would be expected on average in a stream channel would tend to underestimate the erosion parameters. On the other hand, researchers have argued that channel erosion is not caused by the average shear stress but by turbulent fluctuations two to three times the average (Lavelle and Mofjeld, 1987).

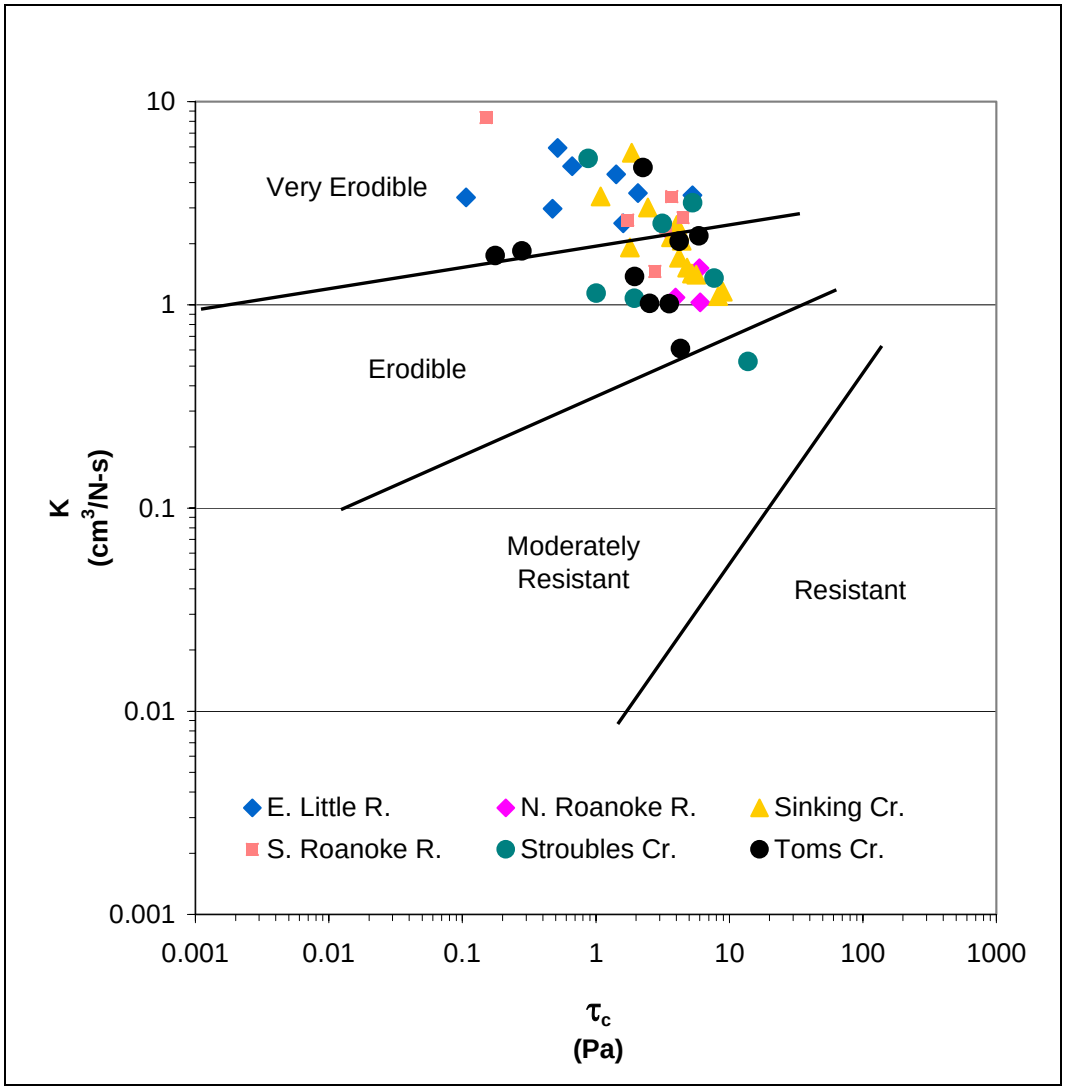


Figure 5.10. Classification of stream bank materials following Hanson and Simon (2001).

Tables 5.3 – 5.6 show the mean, median, and range of data for the soil, root, and stream water parameters for the individual jet tests. These values are typical of riparian soils and streams in the Appalachian Mountains. The area is dominated by limestone geology, so the streams tend to have high pH and electrical conductivities. Total suspended soils are generally low except during runoff events. The unusually low bulk density (0.38 g/cm$^3$) and high moisture contents (215%) were measured along the lower bank of SR3. This site has soils dominated by very fine sands that become suspended during flood events. Due to high water levels at the time

Table 5.3. Mean, median and range of soil properties from individual jet test runs along headwater streams in southwest Virginia.

| | $K_d$* ($cm^3$/N-s) | $\tau_c$ + (Pa) | Aggregate Stability | Bulk Density ($g/cm^3$) | Specific Gravity | Initial Moisture Content | Organic Carbon (%) | Liquid Limit | Plastic Limit | Plasticity Index |
|---|---|---|---|---|---|---|---|---|---|---|
| **Mean** | 2.78 | 3.51 | 0.80 | 1.21 | 2.54 | 0.38 | 1.68 | 0.357 | 0.226 | 13 |
| **Median** | 1.88 | 1.74 | 0.84 | 1.22 | 2.55 | 0.33 | 1.43 | 0.344 | 0.217 | 12 |
| **Minimum** | 0.18 | 0.00 | 0.32 | 0.38 | 2.19 | 0.15 | 0.13 | 0.229 | 0.152 | 4 |
| **Maximum** | 13.08 | 21.90 | 1.00 | 1.59 | 2.70 | 2.15 | 6.61 | 0.573 | 0.400 | 35 |

* $K_d$ = soil erodibility

+ $\tau_c$ = soil critical shear stress



Table 5.4. Mean, median and range of root length density and root volume ratio from individual jet test runs along headwater streams in southwest Virginia.

| | Very Fine RLD* ($cm/cm^3$) | Fine RLD ($cm/cm^3$) | Small RLD ($cm/cm^3$) | Medium RLD ($cm/cm^3$) | Large RLD ($cm/cm^3$) | Very Fine RVR+ $x10^3$ ($cm^3/cm^3$) | Fine RVR $x10^3$ ($cm^3/cm^3$) | Small RVR $x10^3$ ($cm^3/cm^3$) | Medium RVR $x10^3$ ($cm^3/cm^3$) | Large RVR $x10^3$ ($cm^3/cm^3$) |
|---|---|---|---|---|---|---|---|---|---|---|
| **Mean** | 1.723 | 1.385 | 0.070 | 0.006 | 0.001 | 1.304 | 7.535 | 4.419 | 2.245 | 1.238 |
| **Median** | 0.905 | 1.025 | 0.050 | 0.000 | 0.000 | 0.749 | 5.635 | 3.165 | 0.091 | 0.000 |
| **Minimum** | 0.010 | 0.010 | 0.000 | 0.000 | 0.000 | 0.008 | 0.031 | 0.000 | 0.000 | 0.000 |
| **Maximum** | 16.68 | 6.41 | 0.490 | 0.070 | 0.030 | 12.581 | 42.968 | 37.649 | 27.010 | 43.489 |

* RLD = root length density

+ RVR = root volume ratio

Table 5.5. Mean, median and range of water physical and chemical characteristics for individual jet test runs in headwater streams in southwest Virginia.

| | Water Temperature ($^{o}$C) | Water Conductivity (μS/cm) | Water pH | Total Suspended Solids (mg/l) |
|---|---|---|---|---|
| **Mean** | 18.3 | 302 | 8.1 | 10.3 |
| **Median** | 18.5 | 260 | 8.1 | 5.6 |
| **Minimum** | 12.5 | 62 | 7.5 | 0.4 |
| **Maximum** | 22.0 | 650 | 8.5 | 37.5 |



Table 5.6. Mean, median and range of soil chemistry and texture for upper and lower banks from composite samples along headwater streams in southwest Virginia.

| | Soil pH | Soil Conductivity (μS/cm) | $K^{+}$ ($cmol_c$ /kg) | $Mg^{2+}$ ($cmol_c$ /kg) | $Ca^{2+}$ ($cmol_c$ /kg) | $Na^{+}$ ($cmol_c$ /kg) | Pore Water Salt (N) | KIF* | $SAR^{+}$ | % Sand | % Silt | % Clay |
|---|---|---|---|---|---|---|---|---|---|---|---|---|
| **Mean** | 7.20 | 841 | 0.006 | 0.114 | 0.216 | 0.028 | 0.008 | 0.068 | 0.58 | 60.68 | 30.7 | 8.7 |
| **Median** | 7.36 | 730 | 0.004 | 0.109 | 0.216 | 0.023 | 0.007 | 0.048 | 0.51 | 58.65 | 30.4 | 7.6 |
| **Minimum** | 5.63 | 340 | 0.001 | 0.011 | 0.018 | 0.016 | 0.002 | 0.010 | 0.22 | 29.5 | 13.5 | 0.2 |
| **Maximum** | 8.17 | 1800 | 0.030 | 0.251 | 0.715 | 0.075 | 0.022 | 0.281 | 1.24 | 83.3 | 54.4 | 31.6 |

* KIF = potassium intensity factor

$^{+}$ SAR = sodium adsorption ratio

of testing, testing along the lower bank of SR3 was conducted below water level. For these reasons, the moisture contents and bulk densities for these tests were outside the typical range of the data. Also, moisture content is expressed on a dry soil mass basis, so the moisture content values appear large.

*5.2.1. Regression Analysis of Overall Data Set*

As an initial step to the regression analyses, correlation between the parameters was investigated by calculating Pearson's correlation coefficient. Table H7 shows Pearson's r for the entire data set with the corresponding p-value. For clarity, only those coefficients greater than 0.4 with p-values less than 0.05 are shown. Results of this analysis indicated soil erodibility was negatively correlated to bulk density (BD; r = -0.57, p = 0.00) and the soil silt+clay content (S+C; r = -0.48, p = 0.00). Soil $K_d$ is positively related to the soil sand content (Sand; r = 0.46, p = 0.00), the ratio of the soil EC to the water EC (SWEC; r = 0.55, p = 0.00), and to the average duration the stream bank was frozen over the previous winter (ADF; r = 0.41, p = 0.02).

As with $K_d$, the soil critical shear stress was correlated to several soil properties. The $\tau_c$ increased with increasing BD (r =0.60, p = 0.00), soil S+C (r = 0.48, p = 0.00), and grain size standard deviation ($\sigma$; r = 0.44, p = 0.00). Conversely, increases in soil sand content (r = -0.49, p = 0.00), the median grain size ($D_{50}$; r = -0.50, p = 0.00), the SWEC (r = -0.45, p = 0.00), and the soil potassium intensity factor (KIF; r = -0.45, p = 0.00), were correlated with decreases in $\tau_c$.

To evaluate the influence of each parameter and to check for nonlinear relationships, $K_d$ and $\tau_c$ were plotted versus each transformed and normalized parameter. Results showed both $K_d$ and $\tau_c$ were linearly related to several parameters. The significance of these observations was checked by conducting both least-squares and Theil-Sen regression. While Theil-Sen regression does not provide a coefficient of determination ($r^2$), it will determine if there is a significant linear relationship between two variables. Theil-Sen regression is a particularly useful analysis for environmental data where outliers are common (Helsel and Hirsch, 1992). Tables 5.7 and 5.8 list those explanatory parameters with a significant impact on $K_d$ and $\tau_c$, respectively.

Soil BD appeared to have the greatest influence on both $K_d$ and $\tau_c$, explaining over 30% of the variance in each erosion parameter. Soil $K_d$ is inversely related to BD, while $\tau_c$ is positively related to BD. These results confirm field observations that little scour occurred

Table 5.7. Single explanatory variables for soil erodibility, $K_d$, with all data (data normalized and transformed, as indicated by subscript "NT").

| Normalized, Transformed Explanatory Parameter | Theil-Sen Slope | Theil-Sen Intercept | Theil-Sen p-value | Least Squares Slope | Least Squares Intercept | Least Squares p-value | Least Squares $r^2$ |
|---|---|---|---|---|---|---|---|
| Bulk density (BD) | -0.60 | 0.21 | 0.000 | -0.57 | 0.00 | 0.000 | 0.327 |
| Soil:Water electrical conductivity (SWEC) | 0.58 | -0.11 | 0.000 | 0.55 | 0.00 | 0.000 | 0.305 |
| Silt+Clay content (S+C) | -0.35 | 0.17 | 0.028 | -0.48 | 0.00 | 0.001 | 0.229 |
| Sand content (Sand) | 0.35 | 0.18 | 0.023 | 0.46 | 0.00 | 0.001 | 0.213 |
| Average duration frozen (ADF) | 0.31 | -0.01 | 0.014 | 0.33 | 0.03 | 0.015 | 0.168 |
| Median grain size ($D_{50}$) | 0.42 | 0.18 | 0.013 | 0.39 | 0.00 | 0.006 | 0.155 |
| Potassium influence factor (KIF) | 0.40 | 0.45 | 0.010 | 0.35 | 0.00 | 0.013 | 0.126 |
| Grain size std. deviation ($\sigma$) | -0.40 | 0.09 | 0.009 | -0.33 | 0.00 | 0.022 | 0.109 |
| Silt:Clay ratio (S:C) | 0.28 | -0.09 | 0.060 | 0.28 | 0.00 | 0.052 | 0.080 |
| Total duration frozen (TDF) | 0.29 | 0.14 | 0.050 | 0.19 | 0.03 | 0.175 | 0.055 |
| Clay activity (CA) | 0.42 | -0.42 | 0.019 | 0.20 | -0.36 | 0.201 | 0.052 |

during jet tests on high density soils. As can be seen in Table H7, several of the other significant explanatory parameters were strongly correlated to BD, including soil texture, soil organic carbon content (OC), SWEC, and KIF. Bulk density was negatively correlated with soil OC ($r = -0.67$, $p = 0.00$), soil sand content ($r = -0.68$, $p = 0.00$), $D_{50}$ ($r = -0.65$, $p = 0.00$), SWEC ($r = -0.69$, $p = 0.00$), and KIF ($r = -0.40$, $p = 0.01$), but was positively correlated to soil $\sigma$ ($r = 0.53$, $p = 0.00$), and the silt+clay content ($r = 0.68$, $p = 0.00$). Bulk density was also slightly correlated

to the ratio of soil pH to water pH (SWpH), as well as to root length density and root volume ratio. It is likely that BD was the most significant explanatory parameter for both $K_d$ and $\tau_c$ because it has low relative variability and measurement error. Also, it is a composite soil parameter that incorporates the impact of several soil properties, including soil texture, soil chemistry, root density, and soil organic matter.

Table 5.8. Single explanatory variables for soil critical shear stress, $\tau_c$, with all data (data normalized and transformed, as indicated by subscript "NT").

| Normalized, Transformed Explanatory Parameter | Theil-Sen Slope | Theil-Sen Intercept | Theil-Sen p-value | Least Squares Slope | Least Squares Intercept | Least Squares p-value | Least Squares $r^2$ |
|---|---|---|---|---|---|---|---|
| Bulk density (BD) | 0.59 | -0.07 | 0.000 | 0.60 | 0.00 | 0.000 | 0.355 |
| Median grain size ($D_{50}$) | -0.53 | 0.03 | 0.001 | -0.50 | 0.00 | 0.000 | 0.250 |
| Sand content (Sand) | -0.47 | 0.06 | 0.001 | -0.49 | 0.00 | 0.000 | 0.240 |
| Silt+Clay content (S+C) | 0.50 | 0.06 | 0.001 | 0.48 | 0.00 | 0.001 | 0.231 |
| Soil:Water electrical conductivity (SWEC) | -0.50 | 0.13 | 0.001 | -0.45 | 0.00 | 0.001 | 0.205 |
| Potassium influence factor (KIF) | -0.45 | 0.16 | 0.001 | -0.45 | 0.00 | 0.001 | 0.199 |
| Grain size std. deviation ($\sigma$) | 0.46 | 0.03 | 0.001 | 0.44 | 0.00 | 0.002 | 0.194 |
| Organic carbon (OC) | -0.31 | 0.22 | 0.013 | -0.34 | 0.00 | 0.019 | 0.114 |
| Total suspended solids (TSS) | -0.29 | 0.07 | 0.032 | -0.25 | 0.00 | 0.089 | 0.062 |
| Very fine root length density (VFRLD) | -0.25 | 0.09 | 0.054 | -0.23 | 0.00 | 0.119 | 0.052 |

In addition to measures of soil density, the SWEC and KIF also explained some variability in $K_d$ and $\tau_c$ (Tables 5.7 – 5.8). Changes in SWEC explained 30% of the variance in $K_d$ and 21% of the variance in $\tau_c$, while KIF accounted for 13% and 20% of the variance in $K_d$ and $\tau_c$, respectively. Increases in SWEC and KIF corresponded to increasing $K_d$ and decreasing $\tau_c$. As discussed in Section 2.2.1, when a soil with a large quantity of interlayer cations is exposed to a fluid with low cation concentrations, water will enter the clay layers due to osmotic differences, causing the clay soils to expand and reducing interparticle attraction. High SWEC ratios indicate the potential for such swelling to occur. High KIF values are indicative of soils derived from both primary micas and fine-grained micas, such as illite (Brady, 1984). The soils from this study with high KIF values were typically friable and easily eroded.

Soil freezing appeared to play a role in stream bank erodibility: increases in both ADF and TDF resulted in increases in $K_d$. This supported research by Asare et al. (1997) that indicated freeze-thaw cycling reduces soil strength. Similar regression relationships existed between $K_d$ and S:C and $K_d$ and TDF. This is unsurprising since S:C and TDF are slightly correlated ($r = 0.40$, $p = 0.02$) and soils high in silt are prone to disruptions by freeze-thaw cycling (Gatto and Ferrick, 2002).

It is interesting to note that increases in very fine root length density (VFRLD) were correlated to decreases in $\tau_c$. This may have resulted from negative correlations between BD and root length density ($r = -0.40$ to $-0.48$, $p = 0.00$ to $0.01$) and between BD and root volume ratio ($r = -0.44$ to $-0.46$, $p = 0.00$), as shown in Table H7. Additionally, VFRLD was positively correlated to soil sand content ($r = 0.40$, $p = 0.01$) and the SWEC ($r = 0.50$, $p = 0.00$), both of which were inversely related to $\tau_c$.

Stepwise multiple linear regression was used to develop predictive relationships for both $K_d$ and $\tau_c$. Due to problems with sensor malfunction and frost heave during the winter of 2002-2003, several of the sites did not have a complete data record. Additionally, water temperature (WT) was not recorded for each jet test due to equipment failure and some soils were nonplastic. Because each site did not have a complete data record, stepwise regression was initially conducted without the parameters WT, plasticity index (PI), clay activity (CA), and the freezing parameters: the number of freeze-thaw cycles (FTC); the total duration frozen (TDF); the average duration frozen (ADF);, the skew of the distribution of the freezing event durations

(Skew); and the relative difference between the average and median freezing durations (RDAM). Following development of a significant relationship using stepwise regression, each of these parameters was added to the regression equation to test their significance. For each statistically significant relationship, the untransformed equation and the original regression equation developed with the normalized, transformed data are shown in brackets with the dimensionless variables marked with the subscript "NT." The normalized, transformed equation was used to discuss the relative significance of the independent parameters, while the standard form of the equation was presented for application. The following relationship was developed for stream bank erodibility (n = 48, p = 0.000, $r^2 = 0.390$):

$$\log(K_d) = 0.52 - 0.31 \cdot BD^{2.5} - 0.06 \cdot \ln(BRVR) \qquad 5.3$$

$$[\, K_{d,NT} = -0.64 \cdot BD_{NT} - 0.26 \cdot BRVR_{NT} \,]$$

where $K_d$ is in $cm^3$/N-s, BD is in $g/cm^3$, and BRVR is the root volume ratio in $cm^3/cm^3$ for all roots with diameters of 2 mm to 20 mm. The coefficients were all significant at $\alpha = 0.05$. While the relationship explained only 39% of the variance in $K_d$, it was highly significant.

This equation indicates that soil erodibility decreased with increased BD and BRVR (Figure 5.11). Also, because the coefficient for $BRVR_{NT}$ was over 50% less than the coefficient for $BD_{NT}$ and BD was raised to the 2.5 power, it appears BD had a much greater influence on $K_d$ than BRVR. It should also be noted that there was no significant correlation between BD and BRVR (Table H7). A highly significant relationship for $\tau_c$ was also developed (n = 42, p = 0.000, $r^2 = 0.569$):

$$\tau_c^{0.36} = 1.79 + 0.47 \cdot BD^{2.5} - 0.27 \cdot \ln(KIF) - 0.85 \cdot SWpH^6 - 0.08 \cdot WT \qquad 5.4$$

$$[\, \tau_{c,NT} = 0.56 \cdot BD_{NT} - 0.44 \cdot KIF_{NT} - 0.33 \cdot SWpH_{NT} - 0.32 \cdot WT_{NT} \,]$$

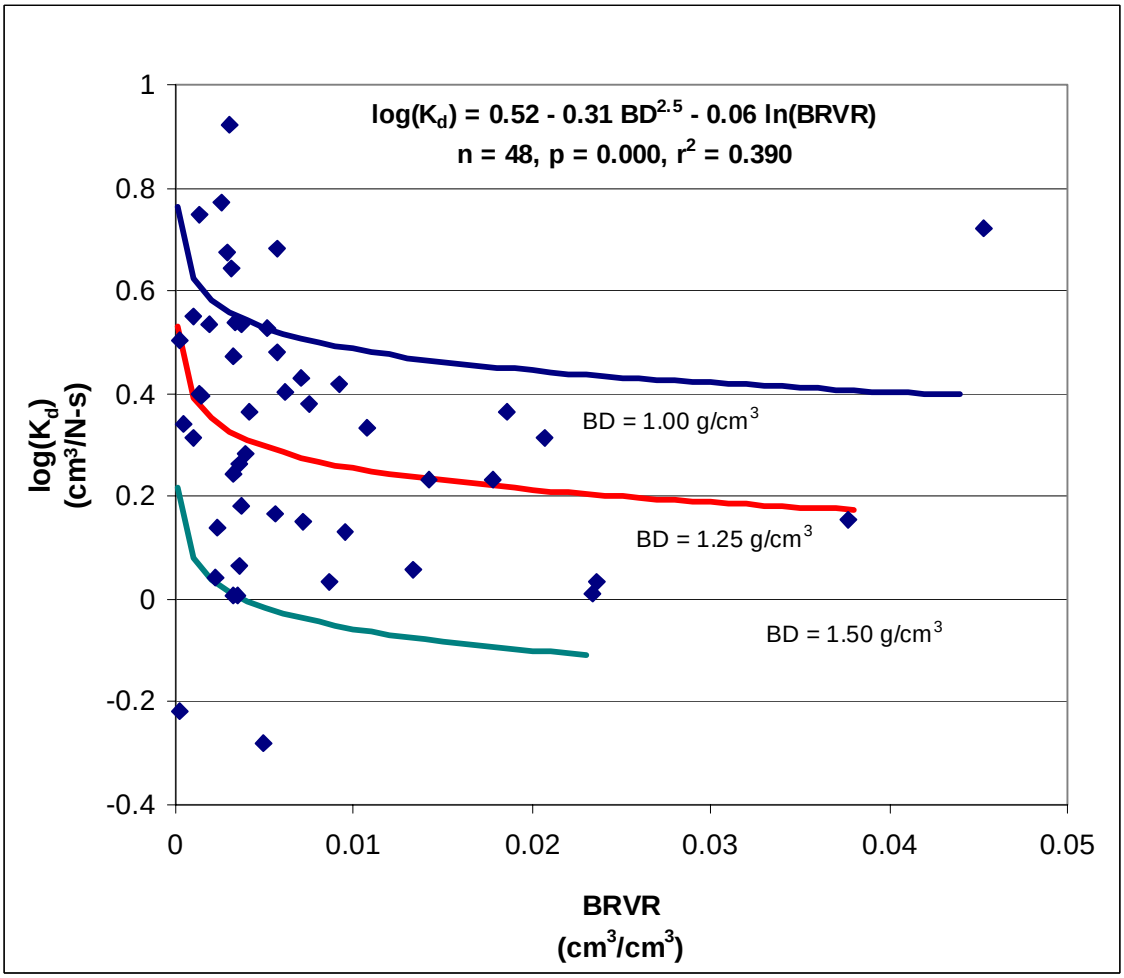


Figure 5.11. The effects of big root volume (2 mm < diameter < 20 mm) and bulk density on soil erodibility for headwater stream banks in southwestern Virginia.

where $\tau_c$ is in Pa, and WT is in degrees Celsius. All of the coefficients were significant at $\alpha$ = 0.05. As with $K_d$, $\tau_c$ was strongly influenced by BD: increases in BD resulted in increases in $\tau_c$ and the coefficient for $BD_{NT}$ was greater than the other parameter coefficients. This relationship also shows that stream and soil chemistry significantly impacted the susceptibility of stream bank soils to fluvial entrainment.

For the test conditions in this study, increases in water temperature increased the susceptibility of these soils to fluid entrainment. As discussed in Ariathuri and Arulanandan (1978), Kandiah (1974) conducted laboratory erosion tests on soils with 30% illite at various

eroding fluid temperatures. Increases in temperature increased the erosion rate and decreased the soil critical shear stress. The author attributed these results to a reduction in the attraction between clay particles with increasing water temperature (Kandiah, 1974). This finding is supported by the diffuse double-layer theory discussed in Section 2.2.1 (McBride, 1994), which shows that the effective distance of the repulsive surface charge on soil particles increases with increasing temperature (Equation 2.1).

These finding have implications for the effects of urbanization on stream bank erosion. In addition to increasing peak flow rates and flood volumes, areas with large amounts of impervious surface also increase water temperatures. In a study on the effects of urbanization on trout streams in Wisconsin and Minnesota, Wang et al. (2003) showed that the average maximum daily stream temperature was linearly related to the amount of connected impervious cover in the watershed according to the relationship T = 18.94 + 0.25 %IC, where T is the average maximum stream temperature in degrees C and %IC is the percent of connected impervious cover in the watershed ($r^2 = 0.27$). Based on Equation 5.4, even if pre-development peak flows were maintained using stormwater management ponds, increased levels of urbanization would continue to impact bank stability by increasing water temperature and thus reducing $\tau_c$. Using the equation developed by Wang et al (2003)., increasing the amount of connected impervious surface from 2% to 10% would increase average maximum daily water temperature from 19.4$^o$C to 21.4$^o$C. These stream temperatures are within the range of temperatures measured in this study. Assuming median values of BD (1.22 g/cm$^3$), KIF (0.048), and SWpH (0.91) for Equation 5.4, increasing the stream water temperature 2$^o$C could reduce the stream bank critical shear stress 30% (2.3 Pa to 1.6 Pa). While the equation by Wang et al. (2003) and Equation 5.4 have relatively low $r^2$, they give a quantitative estimation of the changes in stream temperature and bank $\tau_c$ that could occur with increased urbanization. Since the equation by Wang et al. (2003) is based primarily on baseflow temperatures, more extreme changes in stream temperatures would likely occur at flood stage, since stream flow during a flood would be dominated by runoff from paved surfaces heated by sunlight.

### *5.2.2. Regression Analysis of Group 1 Data*

Following previous work by Allen et al. (1999), the data were split into groups based on soil physical and chemical parameters. Significant differences in soil properties between the

groups are shown in Table 5.9. While Groups 1 and 2 had similar soil textures, soils in Group 1had higher bulk densities and were less reactive, with lower organic carbon contents, plasticity indices, and specific electrical conductivities. Group 3 soils were nonplastic and had significantly greater amounts of sand and a greater KIF, indicating these soils had mica parent materials. While these soils had the lowest pH and conductivity, the organic carbon contents were not significantly less than soils in Group 2.

As with the overall data set, the Pearson' correlation coefficients for each pairwise comparison were evaluated. These coefficients and each p-value are listed in Table H8. Unlike the overall data set, $K_d$ was correlated only to one parameter: the number of freeze-thaw cycles (FTC). Increases in the number of FTC was positively correlated to increases in soil erodibility ($r = 0.69$, $p = 0.02$). As discussed in Chapter 4, research has shown that multiple FTC reduce aggregate stability and decrease soil shear strength (Mostaghimi et al., 1988; Thorne, 1990; Asare et al., 1997; Eigenbrod, 2003). Because the Group 1 soils were fine grained, they would be more susceptible to degradation by ice segregation within the soil.

In contrast to $K_d$, $\tau_c$ was positively correlated to several soil properties, including BD ($r = 0.65$, $p = 0.00$), specific gravity (SG; $r = 0.54$, $p = 0.02$), $\sigma$ ($r = 0.56$, $p = 0.02$), and S+C ($r = 0.47$, $p = 0.05$). This correlation indicated that the dense, fine-grained soils were less susceptible to erosion. This finding was supported by an inverse relationship to the soil sand content, which indicated that $\tau_c$ decreased with increasing sand content ($r = -0.47$, $p = 0.05$). An inverse relationship also existed between the soil salt content and $\tau_c$ (TS, $r = -0.52$, $p = 0.03$).

For each site, a distribution of freezing period durations was developed. Skew was calculated as the skew for each distribution; large values of Skew occurred for sites that had frequent FTC, as well as long periods when the banks remained frozen. Sites with high Skew values typically had a low ADF and underwent moderate FTC. It is interesting to note that BD was not only correlated with soil texture, but also with the freezing parameter Skew and with the length and volume of roots with diameters of 2 - 20 mm (BRLD and BRVR). It appears that frequent FTC acts to reduce soil density. It is widely held that roots also served to loosen soils. This theory was supported by the inverse relationship between BD and both BRLD ($r = -0.66$, $p = 0.00$) and BRVR ($r = -0.53$, $p = 0.03$).

Table 5.9. Statistically significant differences in median soil properties between the soil groups for stream bank soils along headwater streams in southwest Virginia (differences significant at $\alpha = 0.05$ indicated by different letters).

| Soil Group | BD ($g/cm^3$) | AS | OC (%) | Clay (%) | Silt (%) | $D_{50}$ (mm) | $\sigma$ | PI | Soil pH | Soil EC ($\mu S/cm$) | KIF |
|---|---|---|---|---|---|---|---|---|---|---|---|
| 1 – Plastic, Silty | $1.3^{a}$ | $0.82^{a}$ | $1.1^{a}$ | $7.8^{a}$ | $34.2^{a}$ | $0.068^{a}$ | $9.2^{a}$ | $10^{a}$ | $7.5^{a}$ | $710^{a}$ | $0.04^{a}$ |
| 2 – Plastic, Reactive | $1.2^{b}$ | $0.77^{a}$ | $2.1^{b}$ | $11.3^{b}$ | $33.6^{a}$ | $0.069^{a}$ | $8.3^{a}$ | $15^{b}$ | $7.3^{b}$ | $1150^{b}$ | $0.04^{a}$ |
| 3 – Nonplastic | $1.1^{c}$ | $0.91^{b}$ | $1.4^{b}$ | $2.4^{c}$ | $16.8^{b}$ | $0.152^{b}$ | $4.5^{b}$ | $0^{c}$ | $6.9^{b}$ | $660^{a}$ | $0.07^{b}$ |

Table 5.10. Single explanatory variables for soil erodibility, $K_d$, with Group 1 soils (Group 1 soils have a median plasticity index of 10, with median clay and sand contents of 7.8% and 58.0%, respectively, median bulk density of 1.3 g/cm$^3$, and median electrical conductivity of 710 μS/cm).

| Normalized, Transformed Explanatory Parameter | Theil-Sen Slope | Theil-Sen Intercept | Theil-Sen p-value | Least Squares Slope | Least Squares Intercept | Least Squares p-value | Least Squares $r^2$ |
|---|---|---|---|---|---|---|---|
| Freeze-thaw cycles (FTC) | 0.58 | -0.63 | 0.036 | 0.55 | -0.68 | 0.019 | 0.474 |
| Total duration frozen (TDF) | 0.51 | -0.21 | 0.036 | 0.38 | -0.27 | 0.091 | 0.284 |
| Silt+Clay content (S+C) | 0.93 | -0.97 | 0.014 | 0.63 | -0.78 | 0.120 | 0.144 |
| Sand content (Sand) | -0.80 | -0.89 | 0.025 | -0.55 | -0.73 | 0.120 | 0.144 |
| Clay activity (CA) | 0.49 | -0.45 | 0.045 | 0.32 | -0.38 | 0.136 | 0.133 |
| Median grain size ($D_{50}$) | -0.65 | -0.65 | 0.031 | -0.35 | -0.58 | 0.150 | 0.125 |
| Silt:Clay ratio (S:C) | 0.75 | -0.31 | 0.014 | 0.37 | -0.40 | 0.186 | 0.106 |

As with the overall data set, Theil-Sen and least-squares regression analyses were conducted to evaluate possible linear relationships between $K_d$ or $\tau_c$ and the explanatory parameters. The results of these analyses are shown in Table 5.10 for $K_d$ and in Table 5.11 for $\tau_c$. As can be seen from Table 5.10, $K_d$ for the Group 1 soils was most strongly influenced by FTC and soil texture. Increases in FTC resulted in increases in the rate at which the stream bank soils eroded. Repeated freezing and thawing of the stream bank soil explained 47% of the variance in $K_d$ and gave credence to the theory that subaerial processes increase the susceptibility of soils to erosion by fluvial entrainment. The erosion rate also appeared to increase as the silt content of the soil increased, as evidenced by a positive slope for both Silt+Clay and for Silt:Clay.

As can be seen in Table 5.10, a significant linear relationship existed between $K_d$ and FTC. The following equation was developed for Group 1 data with a complete winter temperature record (n = 11, p = 0.019, $r^2 = 0.474$):

$$\log(K_d) = -0.25 + 0.11 \cdot FTC^{0.5} \qquad 5.5$$

$$[\, K_{c,NT} = -0.68 + 0.55 \cdot FTC_{NT} \,]$$

The intercept and the coefficient for FTC were both significantly different from zero at $\alpha = 0.05$. The single explanatory variable, FTC, explained over 47% of the variance in $K_d$ (Figure 5.12). A subset of the data was created by removing nine measurements without a complete data record (those sites missing freezing and water temperature data). Using this data subset, an alternative regression equation was developed (n = 9, p = 0.007, $r^2 = 0.897$):

$$\log(K_d) = 0.73 + 0.15 \cdot FTC^{0.5} - \frac{0.12}{MC} - 1.46 \cdot D_{50}^{0.25} \qquad 5.6$$

$$[\, K_{d,NT} = -0.75 + 0.77 \cdot FTC_{NT} + 0.41 \cdot MC_{NT} - 0.50 \cdot D_{50,NT} \,]$$

where MC is the antecedent moisture content in decimal notation and $D_{50}$ is the median grain size in mm. The intercept and the coefficients were significant at $\alpha = 0.05$.

Equation 5.6 shows that the erodibility of the Group 1 soils increased with increasing moisture content and decreasing particle size. This finding is opposite of results reported by several researchers who showed that dry soils are more susceptible to erosion due to the effects of soil slaking and desiccation cracking (Grissinger et al., 1963; Grissinger et al., 1981; Allen et al., 1999; Hanson and Cook, 1998). While it is well known that soil shear strength also increases with reductions in soil moisture (Tengbeh, 1993), little correlation has been shown between bulk shear strength and erosion resistance (Arulanandan et al., 1980). On the other hand, increases in soil moisture will result in increased hydration of interlayer cations, which would increase the interlayer spacing of the clay fraction. Greater spacing between clay layers would make the soil

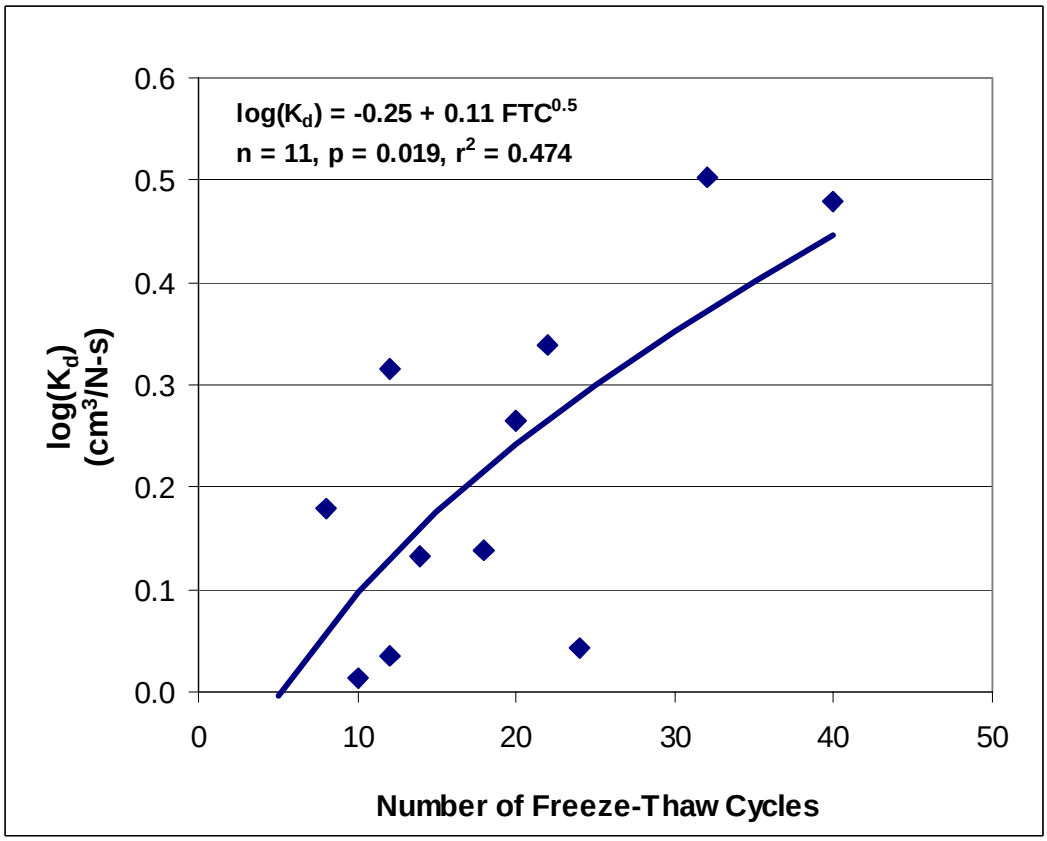


Figure 5.12. Relationship between soil erodibility and the number of freeze-thaw cycles for Group 1 soils (Group 1 soils have a median plasticity index of 10, with median clay and sand contents of 7.8% and 58.0%, respectively, median bulk density of 1.3 g/cm3, and median electrical conductivity of 710 μS/cm).

more susceptible to erosion. Additionally, soils that had higher moisture contents would also be more susceptible to degradation by FTC.

Decreases in $D_{50}$ were also correlated to increases in the erosion rate. This is contrary to a report by Roberts et al. (1998), who showed that the erosion rate of quartz particles increased with increasing particle size in the range of 10 – 100 μm. Even though the $D_{50}$ for Group 1 and Group 2 soils was similar, Group 2 had significantly higher clay contents ($p = 0.02$). Therefore, reductions in $D_{50}$ for Group 1 would indicate increases in the soil silt content. Previous researchers have shown that soil erosion increases with increasing silt content (Wischmeier and Mannering, 1969; Dunaway et al., 1994). Additionally, results from the simple linear regression

analysis showed positive correlation between both S:C and S+C and $K_d$, indicating that increased erosion rates were linked to the silt content of the soil.

This relationship (Equation 5.6) was highly significant and explained almost 90% of the variance in $K_d$. It confirmed that FTC was an important factor in Group 1 soil erodibility, as well as initial soil moisture content and the soil grain size. However, because this relationship was not significant for the entire Group 1 data set, it suggested Group 1 soils may not have been entirely distinct. The only significant difference between the soils in the regression and those removed due to lack of data was in the KIF. The KIF for the sites used in Equation 5.13 had a significantly higher average KIF (0.07) than those removed from the analysis (average KIF = 0.04) at $p = 0.04$. Increases in the ratio of potassium to calcium and magnesium are indicative of soils with mica parent materials, such as illites.

Table 5.11 shows the results of the simple linear regression for $\tau_c$. These results suggest that the critical shear stress for Group 1 soils increased as the grain size decreased. The grain size standard deviation accounted for 31% of the variance in $\tau_c$, while the silt+clay and sand contents each explained 22% of the variance in $\tau_c$. The total salt content of the soil (TS) was also a significant factor: increases in TS decreased $\tau_c$. This finding contradicts results by Arulanandan et al. (1975), who reported increases in $\tau_c$ with increases in pore water salt concentration. The effect they observed was particularly pronounced at low SAR values (1-2). The authors suggested that the higher salt concentrations, particularly of $Ca^{2+}$ and $Mg^{2+}$, caused the soils to flocculate, thus increasing their resistance to erosion. Since remolded samples were used in that study, this explanation is plausible. Because the current study measured $\tau_c$ in situ, flocculation of the soils would not likely be a significant process. Instead, it is likely that increases in soil salt concentrations increased the swelling of soils during testing due to osmotic differences between the soil pore water and the stream water.

Using stepwise multiple linear regression, two significant relationships were developed. The first relationship predicted the $\tau_c$ as a function of $\sigma$ and the soil sand content, while the second used $\sigma$ and BD as the explanatory parameters. This seems reasonable as Table H8 indicates Sand and BD were inversely correlated ($r = -0.57$, $p = 0.01$). The two regression equations were as follows:

Table 5.11. Single explanatory variables for soil critical shear stress, $\tau_c$, with Group 1 soils (Group 1 soils have a median plasticity index of 10, with median clay and sand contents of 7.8% and 58.0%, respectively, median bulk density of 1.3 g/cm$^3$, and median electrical conductivity of 710 μS/cm).

| Normalized, Transformed Explanatory Parameter | Theil-Sen Slope | Theil-Sen Intercept | Theil-Sen p-value | Least Squares Slope | Least Squares Intercept | Least Squares p-value | Least Squares $r^2$ |
|---|---|---|---|---|---|---|---|
| Grain size std. deviation (σ) | 0.58 | 0.02 | 0.025 | 0.63 | -0.02 | 0.016 | 0.311 |
| Total salt content (TS) | -0.36 | 0.49 | 0.045 | -0.37 | 0.29 | 0.028 | 0.268 |
| Silt+Clay content (S+C) | 0.76 | -0.03 | 0.053 | 0.87 | -0.21 | 0.047 | 0.225 |
| Sand content (Sand) | -0.66 | 0.04 | 0.045 | -0.75 | -0.14 | 0.050 | 0.219 |

$$\tau_c^{0.36} = 1.48 + 0.11 \cdot \sigma - 0.00035 \cdot Sand^2 \quad (n = 9,\ p = 0.022,\ r^2 = 0.718), \text{ and} \qquad 5.7$$

$$[\tau_{c,NT} = -0.86 + 0.87 \cdot \sigma_{NT} - 1.33 \cdot Sand_{NT}^2]$$

$$\tau_c^{0.36} = -0.44 + 0.067 \cdot \sigma + 0.64 \cdot BD^{2.5} \quad (n = 18,\ p = 0.001,\ r^2 = 0.663). \qquad 5.8$$

$$[\tau_{c,NT} = -0.60 + 0.52 \cdot \sigma_{NT} + 0.75 \cdot BD_{NT}]$$

where σ is the standard deviation of the grain size distribution and Sand is the soil sand content in decimal notation. The coefficients were significant at $\alpha = 0.05$, except for the intercept of Equation 5.7, which had a p-value of 0.066. Both of these equations were highly significant and explained a large amount of the variance in $\tau_c$. Because the soils in this study contained little or no gravel, soils with high σ were indicative of soils with high clay contents. Equations 5.7 and 5.8 also supported the conclusion from the simple linear regressions that fine grained soils (σ is large and Sand is small) had a greater critical shear stress and were thus more resistant to fluvial entrainment. Previous research has shown that $\tau_c$ increases with increasing clay content (Anderson, 1975; Grissinger et al., 1981; Thorne and Tovey, 1981; Osman and Thorne, 1988;

Gray and Sortir, 1996). Allen et al. (1999) showed that soil erodibility increased with increasing sand content for soils with less than 10% clay.

As with the regression equations for $K_d$, Equation 5.7 changed when applied to the entire data set:

$$\tau_c^{0.36} = 1.36 + 0.078 \cdot \sigma - 0.00018 \cdot Sand^2 \quad (n = 18, p = 0.005, r^2 = 0.508). \qquad 5.9$$

$$[\tau_{c,NT} = -0.39 + 0.60 \cdot \sigma_{NT} - 0.71 \cdot Sand_{NT}]$$

While Equation 5.9 does not explain as much of the variance in $\tau_c$ as Equation 5.9, it is more significant. Additionally, the form of the equation is similar to that of Equation 5.9: the coefficients for $\sigma$ and Sand are positive and negative, respectively.

*5.2.3. Regression Analysis of Group 2 Data*

Group 2 soils differ from Group 1 soils in that they had lower bulk densities and pH, but higher organic carbon contents, plasticity indices, and electrical conductivities (Table 5.9). Evaluation of the Pearson's correlation coefficient for these sites (Table H9) indicates that soil erodibility was correlated only to Skew (r = -0.59, p = 0.05) and soil critical shear stress was correlated only to the total salt concentration (TS; r = -0.52, p = 0.05). This result provides further confirmation that $K_d$ was strongly influenced by repeated soil freezing. The negative correlation between $\tau_c$ and soil salts supports evidence that increasing differences in cation concentration between the soil pore water and the eroding fluid can cause swelling of the clay soils and reduce the energy required to entrain soil aggregates.

Simple linear regression produced only one significant relationship. Using Theil-Sen regression for a subset of the Group 2 soils (sites without freezing or water temperature data removed), produced the following relationship between $K_d$ and FTC:

$$\log(K_d) = 0.53 - 0.094 \cdot FTC^{0.5} \quad (n = 9, p = 0.012) \qquad 5.10$$

$$[K_{NT} = -0.53 - 0.47 \cdot FTC_{NT}].$$

Using stepwise regression for the subset of Group 2 soils where sites without freezing or water temperature data were removed (6 measurements), two highly significant relationships for $K_d$ were developed. In each equation, $K_d$ was a function of the fine root length density (FRLD), the soil pore water salt concentration, and a freezing parameter, either ADF or FTC. The number of FTC and the ADF were highly negatively correlated (r = -0.96, p = 0.00), thus they were interchangeable. The two regression equations are as follows (n = 9, $r^2 = 0.984$, p = 0.000; n = 9, $r^2 = 0.996$, p = 0.000):

$$\log(K_d) = 0.74 - 0.55 \cdot FRLD^{0.25} - 0.059 \cdot FTC^{0.5} - 0.07 \cdot \ln(PW) \qquad 5.11$$

$$[\, K_{d,NT} = -0.11 - 0.37 \cdot FRLD_{NT} - 0.29 \cdot FTC_{NT} - 0.15 \cdot PW_{NT} \,]$$

$$\log(K_d) = 1.00 - 0.58 \cdot FRLD^{0.25} - \frac{1.02}{ADF^{0.2}} - 0.068 \cdot \ln(PW) \qquad 5.12$$

$$[\, K_{d,NT} = -0.09 - 0.39 \cdot FRLD_{NT} + 0.26 \cdot ADF_{NT} - 0.14 \cdot PW_{NT} \,]$$

where FRLD is in $cm/cm^3$ , ADF is in hours, and PW in equivalents/L. The coefficients for all the parameters were significant at $\alpha = 0.05$, except for the intercept for Eqn. 5.11, which was significantly different from zero at p = 0.07. Both of these equations were highly significant and explained over 98% of the variance in $K_d$. Because these equations were developed with a small dataset (n=9), the high $r^2$ values may have been a statistical artifact caused by a number of independent variables and a small dataset. These regression equations suggest that increases in FRLD reduced the rate at which Group 2 stream bank soils eroded. They also confirm previous results that indicated soil freezing and soil cation content influenced soil erodibility.

Contrary to the Group 1 soils, increased FTC resulted in greater soil stability for the Group 2 soils. This finding is consistent with Equation 5.12, which demonstrated a positive relationship between $K_d$ and ADF. Sites with a large ADF typically remained frozen instead of undergoing repeated FTCs. The erosion rate was also negatively correlated with the pore water salt concentration. As discussed in previous sections, differences in ionic strength between the

pore water and the eroding fluid can cause soil swelling, making soils more susceptible to erosion.

It should also be noted that when the sites with missing water temperature data but a complete freezing record (n = 3) were included in the analysis, the coefficients for FTC and ADF were no longer significant at $\alpha = 0.05$. One of those three sites (SR4 lower bank) had an unusually large number of FTC and a very low ADF that strongly influenced the regression relationship. This example showed that while the regression relationships presented were highly significant and explained a large amount of the variance, they were extremely sensitive to individual data points.

While significant relationships were developed for $\tau_c$, the residuals exhibited both strong heteroscedasticity and serial dependence. The lack of conformity to the underlying assumptions of least squares regression lead the author to question the validity of the results and so the equations were not presented. It is not unreasonable to find inconclusive results for the critical shear stress. Some researchers have suggested that a critical shear stress, such as that observed with noncohesive soils, does not exist for cohesive soils (Anderson, 1975; Lavelle and Mofjeld, 1987).

### *5.2.4. Regression Analysis of Group 3 Data*

Evaluation of the Pearson's correlation coefficients for the Group 3 soils (Table H10) revealed that soil erodibility was negatively correlated to BD ($r = -0.72$, $p = 0.00$), big root length density (BRLD; $r = -0.53$, $p = 0.05$), and big root volume ratio (BRVR; $r = -0.64$, $p = 0.01$). As with the Group 2 soils, K was inversely related to root density, suggesting that roots reinforce soils and reduce erosion rates.

Results of the simple linear regression analyses for $K_d$ are shown in Table 5.12. Changes in BD explained over 50% of the variance, while changes in BRVR explained over 40%. While there was a significant nonparametric linear relationship between $K_d$ and SWEC and the TSS concentration of the eroding fluid, neither of these parameters accounted for more than 20% of the variance in $K_d$. Additionally, the slopes were not significantly different from zero: the least-squares regression p-values for these two parameters were greater than 0.10.

Using stepwise multiple linear regression the following two regression equations were developed for $K_d$:

$$\log K_d = 0.45 - 0.11 \cdot \ln BRVR - 0.21 \cdot BD^{2.5} - 0.50 \cdot TS^{0.5}, \text{ and} \quad 5.13$$

$$[K_{d,NT} = 0.27 - 0.49 \cdot BRVR_{NT} - 0.45 \cdot BD_{NT} - 0.31 \cdot TS_{NT}] \text{ (n = 15, p = 0.000, } r^2 = 0.842)$$

$$\log K_d = 0.97 - 0.42 \cdot BD^{2.5} + 0.56 \cdot SWpH^6 - 0.38 \cdot AS^5 \text{ (n = 15, p = 0.000, } r^2 = 0.727), \quad 5.14$$

$$[K_{d,NT} = 0.38 - 0.87 \cdot BD_{NT} + 0.39 \cdot SWpH_{NT} - 0.33 \cdot AS_{NT}]$$

where AS is the aggregate stability in decimal notation. The coefficients were all significant at $\alpha = 0.05$, although the intercepts were not significantly different from zero. Both of these equations were highly significant and explained over 70% of the variation in $K_d$. As with the correlation coefficients and the simple linear regression, this analysis suggests BD played a significant role in $K_d$ for the Group 3 soils: increases in BD resulted in decreases in erosion rate. The erosion rate was also reduced by increases in BRVR (Figure 5.13), TS, and AS, and decreases in SWpH. The reduction in erosion rate due to larger diameter roots (2 mm < D < 20 mm) was likely due to hydraulic impacts of the roots: the larger roots disrupted the flow and reduced near bank shear stresses.

The stream bank soil critical shear stress ($\tau_c$) was positively correlated to BD (r = 0.68, p = 0.01) and negatively related to the SWEC (r = -0.53, p = 0.04), indicating that $\tau_c$ was also influenced by the soil bulk density and differences in the soil pore water and stream water ionic strength. This finding was supported by the simple linear regression results (Table 5.13). Changes in BD explained almost 50% of the variability in $\tau_c$ and both the Theil-Sen and least-squares regressions were highly significant ($p \leq 0.006$). It is interesting to note that $\tau_c$ was also inversely related to very fine root length density and root volume ratio (VFRLD and VFRVR, respectively). While the quantity of roots greater than 2.0 mm in diameter appeared to reduce the erosion rate of Group 3 soils, increases in roots less than 0.5 mm in diameter were inversely correlated to the shear stress required to initiate fluvial entrainment. This relationship to VFRLD (Table 5.12) implies that converting a herbaceous buffer to a forested buffer could increase $\tau_c$ at

Table 5.12. Single explanatory variables for soil erodibility, $K_d$, with Group 3 soils (Group 3 soils are nonplastic with median clay and sand contents of 2.4% and 80.8%, respectively, median bulk density of 1.1 g/cm$^3$, and median electrical conductivity of 660 μS/cm).

| Normalized, Transformed Explanatory Parameter | Theil-Sen Slope | Theil-Sen Intercept | Theil-Sen p-value | Least Squares Slope | Least Squares Intercept | Least Squares p-value | Least Squares $r^2$ |
|---|---|---|---|---|---|---|---|
| Bulk density (BD) | -0.65 | 0.20 | 0.054 | -0.74 | 0.16 | 0.002 | 0.523 |
| Big root volume ratio (BRVR) | -0.95 | 0.66 | 0.001 | -0.80 | 0.75 | 0.010 | 0.411 |
| Soil:Water electrical conductivity (SWEC) | 0.72 | 0.30 | 0.054 | 0.66 | 0.16 | 0.107 | 0.188 |
| Total suspended solids (TSS) | 0.38 | 0.51 | 0.043 | 0.26 | 0.71 | 0.166 | 0.142 |

the stream bank toe from 0.71 Pa to 0.93 Pa (31% increase), assuming a median VFRLD at a depth of 75-90 cm of 0.28 cm/cm$^3$ for a herbaceous buffer and of 0.20 cm/cm$^3$ for a forested buffer (Chapter 3).

Two significant multiple linear regressions were developed for $\tau_c$. The first equation was developed with the entire Group 3 data set and is as follows:

$$\tau_c^{0.36} = -0.24 + 1.26 \cdot BD^{2.5} - \frac{0.23}{MC} - \frac{0.86}{S:C^{0.4}} \qquad (n = 15,\ p = 0.002,\ r^2 = 0.733) \qquad 5.15$$

$$[\ \tau_{c,NT} = 0.46 + 1.48 \cdot BD_{NT} + 0.44 \cdot MC_{NT} + 0.35 \cdot S:C_{NT}\ ]$$

where MC is the antecedent moisture content and S:C is the ratio of silt to clay in the soil. All the coefficients were significant at $p < 0.03$, with the exception of the intercept, which had a p-value of 0.10. The equation was highly significant ($p = 0.002$) and it explained almost 75% of the variance in $\tau_c$. This equation reinforces the importance of BD in $\tau_c$: the coefficient for BD

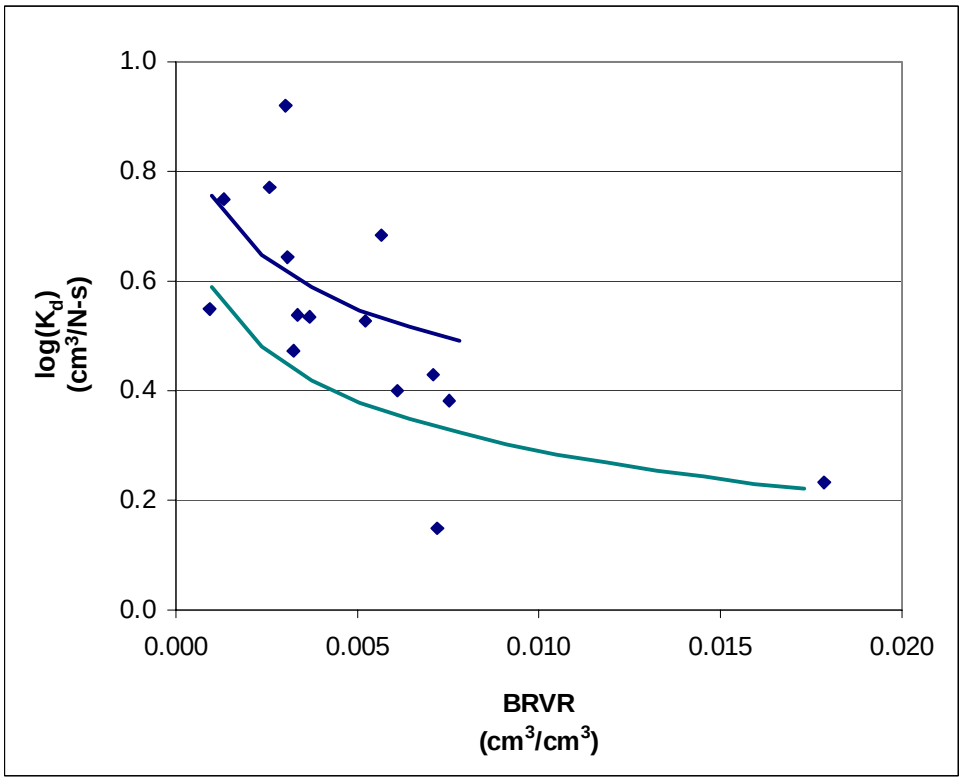


Figure 5.13. The effects of big root volume (2 mm < diameter < 20 mm) and bulk density on soil erodibility of Group 3 soils (Group 3 soils are nonplastic with a median clay and sand contents of 2.4% and 80.8%, respectively, median bulk density of 1.1 g/cm3, and median electrical conductivity of 660 μS/cm).

was three times the coefficients for MC or S:C. Increases in either the antecedent moisture content or the silt:clay ratio of the soil also increased the stress required to initiate erosion. Increases in moisture content may have reduced soil entrainment by decreasing slaking or by increasing soil cohesion from moisture films on the soil particles. The increase in $\tau_c$ with increasing silt:clay ratio contradicts findings by previous researchers that soil erosion increases with increasing silt content (Wischmeier and Mannering, 1969; Dunaway et al., 1994). Elliot et al. 1990 reported a positive correlation between silt content and $\tau_c$. The authors did not feel this positive correlation represented physical reality; they attributed it to a flaw in the method used to determine $\tau_c$. One method of determining $\tau_c$ is to plot the erosion rate versus the applied shear stress as a linear function. The intercept of the line (erosion rate of zero) is then taken as $\tau_c$. Because silty soils erode rapidly, when the erosion rate is plotted versus the applied shear stress,

Table 5.13. Single explanatory variables for soil critical shear stress, $\tau_c$, with Group 3 soils (Group 3 soils are nonplastic with a median clay sand contents of 2.4% and 80.8%, respectively, median bulk density of 1.1 g/cm$^3$, and median electrical conductivity of 660 μS/cm).

| Normalized, Transformed Explanatory Parameter | Theil-Sen Slope | Theil-Sen Intercept | Theil-Sen p-value | Least Squares Slope | Least Squares Intercept | Least Squares p-value | Least Squares $r^2$ |
|---|---|---|---|---|---|---|---|
| Bulk density (BD) | 0.92 | 0.28 | 0.004 | 0.88 | 0.29 | 0.006 | 0.456 |
| Soil:Water electrical conductivity (SWEC) | -1.07 | 0.83 | 0.054 | -1.03 | 0.51 | 0.042 | 0.281 |
| Very fine root length density (VFRLD) | -0.74 | -0.17 | 0.026 | -0.72 | -0.25 | 0.060 | 0.246 |
| Very fine root volume ratio (VFRVR) | -0.71 | -0.14 | 0.054 | -0.74 | -0.26 | 0.062 | 0.242 |

the resulting line has a steep slope and a large extrapolated intercept. Considering that $\tau_c$ in this study was determined by fitting a logarithmic hyperbolic function to the data (following Blaisdell et al., 1981) to estimate $H_e$, rather than a straight line (see discussion in Section 2.2.3), it appears that the increase in $\tau_c$ with increasing silt content may have physical merit. In sandy soils, the smaller silt particles may fill interstitial spaces, reducing the void ratio and fluid entrainment.

Three of the sites in the Group 3 soil data set did not have a complete winter temperature record. Because of this, a stepwise multiple linear regression analysis was also conducted on a subset of the Group 3 soils data. This analysis produced the following equation (n = 12, p = 0.001, $r^2 = 0.913$):

$$\tau_c^{0.36} = 2.11 + 2.21 \cdot AS^5 - 1.07 \cdot RDAM^2 - 1.15 \cdot SWpH^6 - 0.00044 \cdot SG^8 \qquad 5.16$$

$$[\tau_{c,NT} = -0.59 + 1.07 \cdot AS_{NT} - 0.54 \cdot RDAM_{NT} - 0.45 \cdot SWpH_{NT} - 0.35 \cdot SG_{NT}]$$

where RDAM is the ratio of the average duration frozen to the median duration frozen and SG is the soil specific gravity. All the regression coefficients were significant at $\alpha = 0.05$. This relationship explained the majority of the variance in $\tau_c$ and was highly significant. The coefficient for AS is almost double the coefficients for the remaining parameters, indicating increases in AS resulted in significant increases in $\tau_c$. RDAM is a parameter that indicates the relative difference between the average and median durations frozen; high values of RDAM are indicative of sites that underwent frequent FTC but also had extended periods where the stream banks remained frozen. Increases in bank freezing appeared to decrease $\tau_c$. As with $K_d$, differences in soil and stream chemistry influenced $\tau_c$: large differences between the soil pore water pH and the stream pH reduced the energy required to initiate erosion.

It is interesting to note that $\tau_c$ decreased with increases in SG. Since these soils are noncohesive, particle entrainment is a function of force balances on individual soil grains. High values of SG would be indicative of dense particles that would be difficult to entrain. This seemingly contradictory result may be because SG is highly correlated with soil total salts (TS; Table H10: $r = -0.78$, $p = 0.00$). Substituting TS into equation 5.16 for SG also produced a highly significant regression relationship with similar $r^2$, but the coefficients for TS and SWpH were significant at $p = 0.06$. Because SG can be measured with greater accuracy than TS, it is likely that it had less error and thus was more significant in the regression equation.

## 5.3 Discussion

### *5.3.1. Bulk Density*

The most important factor determining the soil erosion rate in this study was bulk density. Increases in bulk density resulted in decreases in soil erodibility and increases in the critical shear stress for the overall data set, as well as for Group 1 and Group 3 soils. Bulk density explained 33% and 52% of the variance in $K_d$ and 36% and 46% of the variance in $\tau_c$ for the overall and Group 3 soils, respectively. Previous researchers reported that soil erosion rates decreased with increasing bulk density (Hanson and Robinson, 1993; Roberts et al., 1998; Allen et al., 1999). Allen et al. (1999) conducted regression analyses to develop predictive equations for the jet index from submerged jet testing (ASTM, 1999). For soils with more than 10% clay,

but clay activities less than 1.25, the jet index was a function of the soil bulk density, clay content, and plastic limit ($r^2 = 0.96$). These soils are similar to the Group 1 soils in this study.

It is likely that BD was the most significant explanatory parameter for both $K_d$ and $\tau_c$ because it had relatively low variability and measurement error. Also, BD is a composite soil parameter that incorporates the impact of several soil properties, including soil texture, soil chemistry, root density, and soil organic matter content. As Grissinger (1982) discussed in a summary of the erosion of cohesive soils, bulk density implies an average interparticle or interlayer distance. Soils with low interparticle distances are less susceptible to swelling and erosion upon wetting.

### *5.3.2. Moisture Content and Aggregate Stability*

The impact of antecedent moisture content (MC) on soil erosion in this study varied with soil type. For the fine grained soils in Group 1, $K_d$ increased with increasing moisture content. This could have been caused by increases in interlayer spacing in the clays with increased soil moisture content (McBride, 1994). Increases in interlayer spacing reduce the strength of cohesive soils and make them more susceptible to erosion (Paaswell, 1973). Additionally, the fact that soil erodibility for the Group 1 soils was positively correlated to FTC and MC, but negatively correlated to $D_{50}$ suggests that FTC played a major role in the erosion of these fine grained soils. Low values of $D_{50}$ were indicative of soils that had a high silt content and thus were more susceptible to ice segregation during freezing. These results support findings by Nearing et al. (1988) that freezing is the primary destabilizing factor for soils.

For the noncohesive soils in Group 3, the critical shear stress increased with increasing MC. This suggests that water films in the soil increased soil cohesion, or that the coarser soils were more susceptible to slaking than the fine grained soils. During the course of the study, the author noted that the stream banks with high sand contents were very friable when dry, suggesting that the former was most likely explanation of the inverse relationship between $\tau_c$ and MC. This observation was confirmed by the study results for aggregate stability. Aggregate stability played a significant role in the erosion of Group 3 stream banks. Increases in AS decreased $K_d$ and increased $\tau_c$. Despite the fact that the Group 3 soils had significantly lower clay contents, as compared to soils in Groups 1 and 2 ($p = 0.0001$), the Group 3 soils had significantly greater dry aggregate stabilities ($p = 0.01$). Since slaking is a major cause of

aggregate instability (Le Bissonais, 1996), the fact that the coarser soil had greater aggregate stability suggests that soil slaking was not significant for the Group 3 soils and that the soil moisture stabilized the sandy stream banks through increases in soil cohesion.

### *5.3.3. Soil Chemistry*

The results of this study provided strong evidence that the interaction of stream and soil chemistry significantly impacts stream bank erosion. For the overall data set, this study showed that increases in both the KIF and the SWpH were correlated to declines in $\tau_c$. High KIF values are indicative of soils derived from both primary micas and fine-grained micas, such as illite (Brady, 1984). The soils from this study with high KIF values were typically friable and easily eroded. The soils along the East Fork of the Little River were so high in primary mica that they glittered.

Increases in the ratio of the soil pH to the stream pH resulted in decreases in $\tau_c$ for the overall data set and for the Group 3 soils. Additionally, soil erodibility for the Group 3 soils increased as the SWpH increases. Previous research has shown that both soil and stream pH influence soil erosion (Grissinger, 1982). Soils become more dispersive with increases in pH, due to increases in pH-dependent CEC (McBride, 1994). Increases in CEC with pH increase surface charge on the soil colloids, leading to greater repulsion between soil particles (McBride, 1994). This increase in CEC with pH is particularly important for soils with significant amounts of pH-dependent charge, such as kaolinites and illites and soils high in organic matter (Grissinger, 1982; McBride, 1994). The clay activity is indicative of the type of clay (Table 5.2); considering the CA for the soils in this study had a median value of 1.3, with a range of 0.7 - 2.6, it appears that illites were one of the dominant clay minerals in these soils. Additionally, the Group 3 soils had significantly more organic carbon than the Group 1 soils.

The soil salt concentration, expressed in units of normality (PW) or mg/kg (TS), also had a significant impact on $K_d$ for the Group 2 and Group 3 soils, respectively. Increases in soil salt concentrations decreased soil erodibility. Additionally, some positive correlation was shown between TS and $\tau_c$ for the Group 3 soils ($p = 0.06$ for TS coefficient). Similar results were reported by Arulanandan et al. (1980) for a flume study on the erosion of cohesive soils. As discussed in McBride (1994), the flocculation of suspended particles increases with increasing

cation charge and concentration; the solution cations reduce repulsion between the negatively charged soil particles.

Considering that the $\tau_c$ and $K_d$ reported in this study were determined using stream water at baseflow conditions, it is likely these parameters will change under flood conditions due to changes in stream water chemistry. During a flood event, the stream pH and EC will decrease while the water temperature will increase. Following equations 5.4, 5.14, and 5.16, these changes in stream water chemistry could result in a decrease in $\tau_c$ and an increase in $K_d$, particularly for soils with illite as the dominate clay mineral.

### *5.3.4. Soil Freezing*

The effects of soil freezing during the previous winter had highly significant effects on both $K_d$ and $\tau_c$ that varied with soil type. Increases in FTC decreased soil erodibility for the Group 1 soils, while increases in RDAM decreased the critical shear stress for the Group 3 soils. These results are supported by previous research (see Chapter 4) that showed soil shear strength and aggregate stability decreased with increased soil FTC (Mostaghimi et al., 1988; Thorne, 1990; Asare et al., 1997; Eigenbrod, 2003).

In contrast to the Group 1 and Group 3 soils, FTC increased soil stability for the Group 2 soils. This finding was confirmed by Equation 5.12, which demonstrated a positive relationship between $K_d$ and ADF. Sites with a large ADF typically remained frozen instead of undergoing repeated FTCs. While research has shown that as many as three FTCs may increase aggregate stability, additional freezing ultimately degrades the soil structure (Lehrsch, 1998; Oztas and Fayetorbay, 2003). Since the soils in Group 2 underwent as many as 28 FTCs, these results cannot be explained by increases in aggregate stability. The inverse relationship between $K_d$ and FTC was likely caused by the removal of interstitial water during soil freezing. The Group 2 soils were distinct from Groups 1 and 3 in that they had significantly higher plasticity indexes, clay activities, electrical conductivities, and sodium contents. These higher values indicate the Group 2 soils were more chemically reactive and had a greater montmorillonite content. As these soils froze, water was removed from the interlayer regions of the clays. This caused the interlayer regions to collapse, increasing soil structure (McBride, 1994). Additionally, because these soils had greater amounts of clay, they were likely less susceptible to damage from ice

formation within the soil because the lower hydraulic conductivities prevented rapid water movement in the soil during freezing.

The strong correlation between soil freezing and soil erosion is somewhat surprising: several bankfull flood events occurred during the late winter and spring of 2003 and several centimeters of bank soil were removed at many sites. These results suggest that the effects of FTC extended beyond the surface soil and affected soil structure within the bank face.

These results also show that the effects of FTC endured over time. These soils were tested one to three months after the last air frost, but FTC was still a significant explanatory parameter for $K_d$. Several researchers have reported decreases in rill erosion rates over time and attributed this to soil consolidation (Nearing et al., 1988; Brown et al., 1989, 1990; West et al., 1992). Further study is needed on the effects of subaerial processes on $K_d$ and $\tau_c$ and temporal changes in these parameters.

*5.3.5. Root Density*

Root density appeared to have a significant impact on stream bank erosion. Based on equations 5.3, 5.11, 5.12, and 5.13, increases in the volume of roots with diameters of 2 - 20 mm (BRVR) or the length of roots with diameters of 0.5 – 2.0 mm (FRLD) reduced $K_d$. Several studies have shown that roots increase soil strength through mechanical reinforcement (Waldron and Dakessian, 1981 and 1982; Materechera et al., 1992; Tengbeh, 1993; Mamo and Bubenzer, 2001a, 2001b). In a laboratory study on the effects of live roots on rill erodibility, Mamo and Bubenzer (2001a) measured decreases in $K_d$ of 8-87% for rooted soils over fallow treatments. In a study similar to this one, Kamyab (1991) conducted regression analyses to determine the impact of root density and soil physical properties on soil erosion from three meadow communities in the Sierra Nevada mountains. Significant relationships were determined between the base 10 logarithm of soil loss and fine, coarse, and total root length density. The $r^2$ for the simple linear regressions varied from 0.26 to 0.34. For the Group 3 soils in this study, a similar $r^2$ (0.41) was found between $K_d$ and BRVR. Extending the work of Kamyab, Dunaway et al. (1994) also reported reductions in erosion rates with increases in RVR for wet meadow communities. It should be noted that the coefficients for both BRVR and FRLD were small, indicating soil physical and chemical properties played a greater role in soil erodibility than root reinforcement.

It is interesting to note that $\tau_c$ was inversely related to very fine root length density and root volume ratio (VFRLD and VFRVR, respectively) for the overall data set and for the Group 3 soils. While the quantity of roots greater than 2.0 mm in diameter appeared to reduce the erosion rate of Group 3 soils, increases in roots less than 0.5 mm were negatively correlated to $\tau_c$. While it appears contradictory that soil $\tau_c$ would decrease with increasing root density, there was also a significant positive correlation between VFRVR and SWEC for both the overall data set and the Group 3 soils (overall: $r = 0.50$, $p = 0.00$, Table H7; Group 3: $r = 0.60$, $p = 0.02$, Table H10). Increases in the ratio of the soil electrical conductivity to the stream electrical conductivity would suggest soil clays would be more susceptible to expansion due to osmotic swelling. As reported in Chapter 3, the quantity of very fine roots is strongly correlated to the quantity of herbaceous vegetation in the riparian buffer. Areas with large amounts of herbaceous vegetation (golf courses, pastures, meadows, etc.) are more likely to receive fertilizer applications than forested areas and a higher pore water ionic strength would be expected following fertilizer applications.

### *5.3.6. Example Application of Study Results*

This study illustrates that riparian vegetation plays a dual role in stream bank erodibility. While the roots of woody riparian vegetation are important for stream bank stabilization, results of this study also indicated that the presence of mature riparian forests encouraged freeze-thaw cycling and hence may also act to destabilize bank soils. To evaluate the combined effects of these two factors, the study findings were used to estimate the change in soil erodibility at the stream bank toe (75-90 cm depth) that would occur if a grass riparian buffer were converted to a woody buffer, using Equations 5.3, 5.11, 5.12, and 5.13. Due to sampling limitations discussed in Chapter 3, the results of this example are applicable only to relatively steep stream banks with little herbaceous vegetation on the bank face. This bank structure is typically found on the outside of meander bends where there are high hydraulic shear stresses. It is in this region that erosion resistance is of particular concern in stream bank stability.

Using the median aboveground vegetation densities (Table 3.1) and the RLD regression equations presented in Table 3.4, the fine RLD at the bank toe was calculated as 0.138 $cm/cm^3$ and 0.303 $cm/cm^3$ for herbaceous and forested vegetation, respectively. Since there were no significant relationships for the root volume ratio of "big" roots (BRVR; $2 <$ diameter $< 20$ mm),

the median BRVR for the herbaceous and forested sites were used (0.0004 $cm^3/cm^3$ and 0.0029 $cm^3/cm^3$, respectively).

For the overall data set, using the median bulk density value of 1.22 $g/cm^3$ and the median BRVR values in Equation 5.3, the herbaceous and forested erodibilities ($K_{dH}$ and $K_{dF}$) were calculated as 3.02 $cm^3$/N-s and 2.30 $cm^3$/N-s, respectively. These values are similar to the median $K_d$ of 2.17 $cm^3$/N-s. This example implies that converting a herbaceous buffer to a forested buffer would reduce $K_d$ by approximately 24%. Reductions in $K_d$ would decrease the rate at which the stream banks eroded, leading to more stable stream channels under forested vegetation.

To evaluate the impact of changing riparian vegetation on the Group 1 soils, Equation 5.6 was used. The number of freeze-thaw cycles (FTCs) expected under the two cover types were calculated using the first equation in Table 4.3, assuming the BSA values of 0 $m^2$/ha and 34 $m^2$/ha for the herbaceous and forested buffers, respectively (Table 3.1). A median stream depth of 30 cm and a median S+C content of 0.43 for the Group 1 soils were also used. These calculations estimated that the herbaceous stream banks would undergo 15 FTCs in one winter, while the forested stream banks would undergo 23 FTCs. Combining these values with a median moisture content of 0.30 and a median $D_{50}$ of 0.068 mm for the Group 1 soils, the resulting $K_d$ were 1.46 $cm^3$/N-s and 2.01 $cm^3$/N-s for the herbaceous and forested vegetation, respectively. Considering the median $K_d$ for Group 1 was 1.63 $cm^3$/N-s, these values appear to be reasonable estimates of $K_d$. This represents an increase in $K_d$ of 38% due to reforestation of the stream bank. This example illustrates that for soils susceptible to FTC, converting the riparian buffer from a predominately herbaceous cover to a mature forest could increase soil erodibility. It should be emphasized that the riparian forests in this study were deciduous; similar results would not be expected under coniferous forests that maintain a dense canopy throughout the year. Additionally, because dense herbaceous vegetation would likely not develop in the outside of meander bends where the shear stresses are greatest, the reductions in soil erodibility afforded by the herbaceous vegetation would be limited to areas of low shear stress, such as on gently sloping banks along the inside of meander bends. It should also be noted that this evaluation does not consider the hydraulic effects of woody vegetation (namely reductions in near bank shear stress due to increased roughness with woody vegetation). The results of this study do not explicitly indicate that riparian forests should be replaced by herbaceous buffers in high-silt

stream banks. While field observations at the study sites indicated that the dominant bank erosion process under dense forest cover was freeze-thaw cycling, the stream banks under woody vegetation were generally stable, suggesting that the observed stream bank erosion due to subaerial processes was natural and was balanced by sediment deposition within the stream systems.

For the Group 2 soils, $K_d$ was estimated using both FTC and ADF. These parameters were estimated using the equations in Table 4.3, assuming the median vegetation densities in Table 3.4, a stream depth of 30 cm, median S+C and silt contents of 0.44 and 0.34, respectively, for the Group 2 soils, and median values of $53^o$ and 576 m for site aspect and elevation. This estimated the FTCs and an ADF of 15 and 169 hours, respectively, for the herbaceous buffers and 23 and 116 hours, respectively, for the woody buffers. By inputting these values into Equation 5.11 and assuming the values of FRLD calculated from Table 3.4 and a median Group 2 pore water salt concentration (PW) of 0.008 N, $K_{dH} = 3.07$ cm$^3$/N-s and $K_{dF} = 2.44$ cm$^3$/N-s were calculated. These values are similar to the group median $K_d$ of 1.91 cm$^3$/N-s. The change in buffer vegetation would reduce the $K_d$ for the Group 2 soils by 21%, as estimated by Equation 5.11. Repeating these calculations with Equation 5.12 resulted in a $K_{dH}$ of 3.80 cm$^3$/N-s and a $K_{dF}$ of 3.16 cm$^3$/N-s. While these values are higher than those estimated using Equation 5.12, they are well within the range of $K_d$ for the Group 2 soils (0.53 – 5.26 cm$^3$/N-s). Similar to the previous calculations using FTC, the predictions made with ADF indicate that stream reforestation would reduce soil erodibility by 17% for fine grained soils with high plasticity indexes and electrical conductivities.

A similar exercise was conducted for the Group 3 soils, using Equation 5.13. Median group values for bulk density and total salt concentration (1.1 g/cm$^3$ and 0.281 cmol$_c$/kg) were used. The calculations produced a $K_{dH}$ of 6.01 cm$^3$/N-s and a $K_{dF}$ of 3.64 cm$^3$/N-s. These values are similar to the median of 3.41 cm$^3$/N-s and within the range of 1.41-8.35 cm$^3$/N-s for the Group 3 soils. As with the overall data set and the Group 2 soils, converting a herbaceous buffer to a forested buffer would reduce $K_d$ by 39%. Because these soils are coarser than those in Groups 1 and 2, they do not appear to be affected by FTC.

Based on the above analyses, it appears that roots with diameters greater than 0.5 mm act to reinforce stream bank soils and can decrease soil erodibility by as much as 39% for soils that

are not susceptible to FTC. These results confirm findings by Kamyab (1991) that the larger diameter roots are better at reinforcing stream bank soils than the very fine roots. While herbaceous vegetation produces a large quantity of roots, these roots are concentrated in the upper 30 cm of the soil profile and are predominately very fine roots (D < 0.5 mm). As was observed during field testing and confirmed by these analyses, very fine roots do not provide sufficient reinforcement to withstand high hydraulic shear stresses.

*5.3.7. Evaluation of the Jet Test Device*

Observed bank erosion from a single storm event during the study was used to evaluate the ability of the jet test parameters and the excess shear stress equation to predict stream bank erosion. A major storm event occurred on February 22, 2003 following several extended periods of below freezing temperatures. All of the study streams were out of bank and extensive bank erosion occurred at several sites. While measurements of bank erosion were not made as part of this study, the amount of erosion at ST3 due to the February storm was estimated at around 60 cm. This estimate was made based on measurements of bank slope, bank exposure, the distance the soil cores were taken from the original bank face (30 cm), and the post-storm bank geometry in relation to the soil core holes, which were still intact in the dense clay subsoil at this site (Figure 5.14). Considering that the bankfull depth and stream slope at this site are 1.1 m and 0.003, respectively, the maximum channel shear stress was estimated as 33 Pa, using the following equation:

$$\tau_o = \rho g H S \qquad 5.17$$

where ρ is the density of water, g is the acceleration due to gravity, H is the stream depth at bankfull discharge, and S is the stream slope. This simplification of Equation 2.2 assumes that the depth is a good approximation of the hydraulic radius (wide channel) and that the stream bed slope approximates the slope of the energy grade line. Because the stream bank at ST3 is actively eroding and largely devoid of vegetation (i.e. relatively smooth), this equation likely provides a good approximation of actual shear stresses on the bank toe. Applying the excess shear stress equation (Equation 2.7) to the average $K_d$ and $\tau_c$ measured on the lower banks at this site (0.53 $cm^3$/N-s and 13.8 Pa), and assuming that the stream was at bankfull stage for 12-24

Figure 5.14. Soil core holes exposed at site ST3 during February 2003 flood. Bank exposure is approximately 1 m.

hours, the total bank erosion was estimated at 44 – 88 cm. The estimated actual bank erosion of 60 cm was in the center of this range. Considering that several of the parameters used in this simple exercise were grossly estimated, this rough calculation indicated that the submerged jet test device provided adequate measurement of both $K_d$ and $\tau_c$, and that the excess shear stress equation adequately estimated stream bank erosion.

The above comparison also confirms that operating the submerged jet test device at shear stresses well in excess of those applied by the stream did not significantly affect test results. For the streams in this study, bankfull depths ranged from 1.1 to 2.5 m while channel slopes ranged from 0.002 to 0.005. This produced bottom shear stresses in the range of 28 to 71 Pa. The applied shear stresses during testing were in the range of 42 – 273 Pa, well in excess of those

expected at bankfull discharges. As discussed in section 5.2, the test shear stress had little impact on the average site $K_d$ and $\tau_c$

In general, the submerged jet test device was simple to transport, set up, and operate in the field. With a crew of two, three individual runs could be completed in six hours. The greatest problem with the test was undermining of the jet test tank, not so affectionately referred to as "blow-outs." Irregularities in soil structure, rodent burrows, and highly erodible soils were typically causes of test failures due to tank undermining.

It was noted during jet testing that the shape of the scour hole varied greatly between soil types. A wide, shallow scour hole was typically formed during the testing of erosion-resistant soils while a narrow deep scour hole was formed in more erodible soils. Additionally, large woody roots deflected the jet and altered the shape of the scour hole. As noted by Hollick (1976), the shape of the scour hole will affect jet dissipation and should be considered in the analysis of the data. Evaluation of the effects of scour hole shape on jet hydraulics should be conducted.

Grissinger et al. (1981) measured stream bank erosion using an in situ flume. They noted that the erosion varied spatially and temporally and that the soil surface morphology strongly influenced the erosion rate. This suggests that samples on small areas may not be representative of the behavior of entire stream banks under flood conditions. While the jet test device is more portable and easier to setup and run than the flume described by Grissinger et al. (1981), it tests only a small area. Typical scour hole diameters ranged from 2 cm to 10 cm. This small scale may not be large enough to capture differences in surface morphology on some stream banks. In this study, the jet test was incapable of testing heavily forested stream banks, particularly where there was a number of large roots protruding from the bank face (Figure 5.15).

Ultimately, bank erosion predictions based on jet test device measurements and the excess shear stress model should be compared to actual measurements of stream bank erosion to determine the amount of error that could result from model predictions and jet test measurements.

Figure 5.15. Exposed roots at site SR1.

## 5.4. Summary and Conclusions

The soil erodibility ($K_d$) and critical shear stress ($\tau_c$) were measured at 25 field sites using a submerged jet test device. Following testing, soil samples were taken to determine root density and soil bulk density, aggregate stability, Atterberg limits, organic carbon content, specific gravity, and major soil cation concentrations. Soil textural analysis of composite soil samples at each site, as described in Chapter 3, and several freezing parameters (Chapter 4) were also considered. Soil textural properties included the percent of sand, silt, and clay in the soil, as well as the median grain size and the grain size standard deviation. The freezing parameters included the number of freeze-thaw cycles, the total, median, and average duration frozen, the skew of the distribution of freeze-thaw durations, and the relative difference between the average and median durations frozen. Because interactions between the stream and soil chemistry have also been shown to affect soil erosion, stream pH, temperature, and electrical conductivity were measured.

A total of 142 jet test runs were conducted from May through August 2003. Three tests were run on both the upper and lower banks of each site, for a total of six runs per site. The jet test data were analyzed following the procedures described in Hanson and Cook (1997). Test results were averaged across the site to produce a single value for the upper or lower banks. The relative effect of these physical and chemical parameters on $K_d$ and $\tau_c$ was assessed using multiple linear regression on the entire data set as well as subsets of the data. The data were split into subsets based on both soil physical and chemical properties. Both the Group 1 and Group 2 soils were fine grained, but the Group 2 soils were generally more reactive, with higher organic carbon contents, plasticity indexes, and electrical conductivities. The Group 3 soils were nonplastic soils with a large sand fraction and higher KIF values.

Average $K_d$ and $\tau_c$ values ranged from 0.18 – 13.1 $cm^3$/N-s and from 0.0 – 21.9 Pa, respectively. Several highly significant regression relationships were developed that explained 39 – 99% of the variance in the erosion parameters. Results of this study indicated that soil bulk density was the most significant parameter for determining both the erodibility and critical shear stress of stream bank soils: changes in bulk density alone explained 33 – 52% of the variance in $K_d$ and 36 – 46% of the variance in $\tau_c$. Increases in bulk density resulted in decreases in soil erodibility and increases in the critical shear stress. Bulk density was probably an important factor in the determination of the erosion resistance of stream bank soils because it is a composite soil property that incorporates several basic soil properties, such as soil texture, organic matter content, and root density. Additionally, bulk density was relatively easy to measure with accuracy and precision.

This study also showed that increases in both the KIF and the SWpH were correlated to declines in $\tau_c$ for the overall data set and for the Group 3 soils. Additionally, soil erodibility for the Group 3 soil increased as the SWpH increases. Previous research has shown that both soil and stream pH influence soil erosion (Grissinger, 1982). Soils become more dispersive with increases in pH, due to increases in pH-dependent CEC (McBride, 1994). This increase in CEC with pH is particularly important for soils with significant amounts of pH-dependent charge, such as kaolinites and illites and soils high in organic matter (Grissinger, 1982; McBride, 1994).

Increases in the soil salt concentration significantly reduced $K_d$ for the Group 2 and Group 3 soils, respectively. Additionally, some positive correlation was shown between TS and

$\tau_c$ for the Group 3 soils. As discussed in McBride (1994), the flocculation of suspended particles increases with increasing cation charge and concentration; the solution cations reduce repulsion between the negatively charged soil particles.

Considering that the majority of the $\tau_c$ and $K_d$ reported in this study were determined using stream water at baseflow conditions, it is likely these parameters would change under flood conditions due to changes in stream chemistry. During a flood event, the stream pH and EC would decrease while the water temperature would increase. Based on the results of this study, these changes in stream water chemistry would result in a decrease in $\tau_c$ and an increase in $K_d$, making the stream banks more susceptible to erosion.

Soil freezing over the previous winter had significant effects on both $K_d$ and $\tau_c$, depending on soil type. Increases in freeze-thaw cycling resulted in increases in soil erodibility for the Group 1 soils and decreases in the critical shear stress for the Group 3 soils, respectively. In contrast, FTC increased soil stability for the Group 2 soils. This contradiction is likely the result of differences in soil structure; the Group 2 soils were distinct from those in Groups 1 and 3 in that they had significantly higher plasticity indexes, clay activities, electrical conductivities, and sodium contents. These higher values indicated the Group 2 soils are more chemically reactive and had greater montmorillonite content. As these soils froze, water was removed from the interlayer regions of the clays. This caused the interlayer regions to collapse, increasing soil structure (McBride, 1994). By comparison, the Group 1 soils had high silt content and were more susceptible to degradation by ice segregation within the soil. Results of this study also indicated that the effects of FTC were not completely reversed by soil consolidation over time. More information is needed on temporal changes in both $\tau_c$ and $K_d$.

This research provided quantitative evidence of the role of roots in stream bank reinforcement. Study results indicated that $K_d$ of the Group 2 soils was reduced by increases in the length of roots with diameters of 0.5 – 2.0 mm (FRLD), while $K_d$ of the overall data set and the Group 3 soils were decreased by increases in the volume of roots with diameters of 2 - 20 mm (BRVR). As reported in Chapter 3, the quantity of larger diameter roots was positively related to the quantity of woody vegetation in the streamside area. These results imply that roots play a significant role in stream bank erosion and that woody vegetation provides better reinforcement of stream bank soils than herbaceous vegetation due a greater quantity of larger

diameter roots. However, it should be noted that the regression coefficients for both BRVR and FRLD were small, indicating soil physical and chemical properties played a greater role in soil stability than root reinforcement.

While the regression analyses produced several highly significant relationships that explained a large proportion of the data variance, the results were very sensitive to the size of the data set and how the data were segregated. For this reason, the results should be confirmed with additional field data and should be applied only with recognition of this sensitivity. While this sensitivity to soil grouping supported Paaswell's assertion that soils with similar physical and chemical properties will erode by similar means/mechanisms (Paaswell, 1973), more information is needed on the soil properties that indicate the mode of erosion for a given soil. Based on the findings of this study and those of Allen et al. (1999), it appears soil bulk density could be used to provide rough estimates of both soil erodibility and critical shear stress for use in studies of stream bank erosion. It should be recognized, though, that soil chemistry also plays a crucial role in the erosion of stream bank soils.

This study showed the cumulative impacts of riparian vegetation on stream bank erodibility. In addition to reinforcing the stream banks, vegetation affected soil moisture and altered the local microclimate. Using the study results in an example application, it was shown that converting a predominately herbaceous riparian buffer to a forested buffer would reduce soil erodibility by as much as 39% for nonreactive (low plasticity index) soils. Conversely, for a stream composed primarily of silt soils that are prone to freeze-thaw cycling, afforestation could lead to increases in soil erodibility of as much as 38%. It should be emphasized that the riparian forests in this study were deciduous; similar results would not be expected under coniferous forests that maintain a dense canopy throughout the year. Additionally, because dense herbaceous vegetation would likely not develop in the outside of meander bends where the shear stresses are greatest, the reductions in soil erodibility afforded by the herbaceous vegetation would be limited to areas of low shear stress, such as on gently sloping banks along the inside of meander bends. It should also be noted that this evaluation does not consider the hydraulic effects of woody vegetation (namely reductions in near bank shear stress due to increased roughness with woody vegetation). The results of this study do not explicitly indicate that riparian forests should be replaced by herbaceous buffers in high-silt stream banks. While field observations at the study sites indicated that the dominant bank erosion process under dense

forest cover was freeze-thaw cycling, the stream banks under woody vegetation were generally stable, suggesting that the observed stream bank erosion due to subaerial processes was natural and was balanced by sediment deposition within the stream systems.

# Chapter 6. Overall Summary and Conclusions

## 6.1. Summary

According to the U. S. Agricultural Research Service, the physical, chemical, and biological damage of water pollution by sediment costs an estimated $16 billion annually in North America (ARS, 2003). While considerable effort has been directed toward reducing erosion from agricultural and urban lands, a major source of sediment, stream channel degradation, has largely been ignored. Studies have shown that sediment from stream banks can account for as much as 85% of watershed sediment yields and bank retreat rates of 1.5 m - 1100 m/year have been documented (Grissinger et al., 1981; Simon et al., 2000). In addition to water quality impairment, stream bank retreat impacts floodplain residents, riparian ecosystems, bridges, and other stream-side structures (ASCE, 1998).

Stream bank retreat typically occurs by a combination of three processes: subaerial processes, bank erosion, and bank failure (Lawler, 1995). Subaerial processes are climate-related phenomena that reduce soil strength, making it more susceptible to erosion (e.g. frost heave, desiccation cracking) (Thorne, 1982). Erosion is the direct removal of soil particles or aggregates from the stream bed or bank toe by stream flow, while the collapse of stream banks due to slope instability is referred to as bank failure.

Streamside, or riparian, vegetation has a significant impact on stream stability (Thorne and Osman, 1988; USACE, 1994; Abernethy and Rutherfurd, 2000). Viewing stream bank soils as a fiber-reinforced composite material, the roots (fibers) increase the strength of bank soils, making them more resistant to soil erosion and bank failures (Abernethy and Rutherfurd, 2001; Mamo and Bubenzer, 2001). Additionally, vegetation insulates the stream bank from extreme temperature fluctuations, minimizing surface degradation of the bank material by frost heave and desiccation cracking (Thorne, 1990; Abernethy and Rutherfurd, 1998).

While the importance of vegetation in stream bank stability is widely acknowledged, the impacts are complex, poorly understood, and have yet to be quantified (ASCE, 1998). A better understanding of the role of vegetation in stream bank erosion is necessary to improve stream

restoration design, to model the effects of landuse change on channel stability, and to assess the impact of proposed landuse ordinances on water quality (Horwitz et al., 2000).

The overall goal of this research was to compare the effects of woody and herbaceous vegetation on stream bank erosion. This research was intended to quantify the effects of vegetation on subaerial processes and the susceptibility of stream bank material to fluvial entrainment. Specific objectives included the following:

1. Quantify root-length density (RLD) with depth in stream banks as a function of vegetation type and density;
2. Determine the effect of vegetation type on freeze/thaw and desiccation activity; and
3. Quantify the relative effects of vegetation type and root-length density on the erodibility of stream banks in situ using a submerged jet test device.

Twenty-five field sites were established along streams in southwest Virginia. Each site consisted of a 30 meter experimental reach with relatively homogeneous riparian vegetation. The riparian buffers varied from short turfgrass to mature forests, representing the full range of possible vegetation types.

To determine the density and distribution of roots down the bank face, ten 7-cm diameter soil cores were taken by hand corers at each site, in 15 cm increments to a depth of 105 cm. These 10 cores were combined to form a single composite core per site. Subsamples were taken at each increment from the composite core to measure root-length density (the total length of roots per unit volume) and soil particle size distribution with depth. Roots were removed from each sub-sample by hand, washed over a No. 30 (0.5 mm) sieve, and scanned. Root-length was assessed for each of five diameter classes: very fine roots (<0.5 mm), fine roots (0.5-2 mm), small roots (2-5 mm), medium roots (5-10 mm) and large roots (10-20 mm) (Böhm, 1979). Above ground vegetation was sampled using three sets of nested quadrats: tree basal stem area, shrub crown volume, and groundcover biomass were measured within 10 m, 5 m, and 1 m squares, respectively (Bonham, 1989; Davidson et al., 1991). Using K-means cluster analysis, the sites were split into two categories, Forested and Herbaceous, based on aboveground vegetation measurements (Johnson and Wichern, 1992). The aboveground vegetation quantities

and the total RLD for the two vegetation types were compared using the nonparametric Mann-Whitney test.

To determine the effects of vegetation type on freeze-thaw cycling and desiccation cracking, soil temperature (ST, $^{o}$C) and soil water potential (SWP, kPa) were monitored continuously at three sets of paired sites (six sites total) for one year, starting in May 2002. Each pair included one herbaceous riparian buffer and one forested buffer in close proximity along the same stream with similar aspect and soil type. Six sets of Campbell Scientific 107 ST probes and Watermark 200 SWP sensors were installed 1 cm deep in the bank face at each site (Branson et al., 1996). Three sensor sets were installed in the upper bank, 30-45 cm from the top of the bank, at a horizontal spacing of approximately 1 m. Three sensors sets were also placed in the lower bank at distances of 70-100 cm from the top of bank. This monitoring provided an extensive and unique set of stream bank ST and SWP data. Two data periods were analyzed: data collected from June through August were used to evaluate summer conditions, while data from December through February were used to represent winter conditions. Daily minimum and maximum ST, daily ST range, and average daily SWP were compared using a paired-reach approach (Spooner et al., 1985). Additionally, the number of freeze-thaw cycles experienced at each site was determined.

Stream bank erosion rates are frequently modeled using the excess stress equation:

$$E_r = K_d (\tau - \tau_c)^a \qquad 6.1$$

where $E_r$ is the erosion rate (m/s); $K_d$ is the erodibility coefficient ($m^3$/N-s); $\tau$ is the applied shear stress (Pa); $\tau_c$ is the critical shear stress (Pa); and a is a fitted exponent (Hanson and Simon, 2001). The $K_d$ and $\tau_c$ of the stream bank soils were measured in the field using a submerged jet test device (ASTM, 1999). The jet testing device consists of a 12 cm diameter tank that is pounded into the stream bank and filled with water. Stream water is then pumped through a 13 mm diameter nozzle at a constant head, forcing a vertical jet of water against the stream bank. The rate of soil erosion is measured over time using a point gage. Following testing, soil samples were taken to determine root density and soil bulk density, aggregate stability, Atterberg limits, organic carbon content, specific gravity, and sodium adsorption ratio. The effects of aboveground vegetation density, root density, soil freeze-thaw cycling and desiccation, and soil

chemical and physical properties on stream bank erosion were evaluated using multivariate regression techniques.

For both riparian buffer types, roots extended to depths in excess of one meter. At the herbaceous sites, very fine roots (diameter, $D < 0.5$ mm) were most common and over 75% of all roots were concentrated in the upper 30 cm of the stream bank. Under forested vegetation, fine roots ($0.5 \text{ mm} < D < 2.0 \text{ mm}$) were more common throughout the bank profile, with 55% of all roots in the top 30 cm. Overall, the herbaceous sites had significantly greater total RLD ($D < 20$ mm) than forested sites in the top 30 cm ($\alpha = 0.01$). There were no significant differences in RLD for roots greater than 0.5 mm in diameter ($\alpha = 0.05$) between the buffer types at depths of less than 30 cm, while greater depths, the forested sites had significantly greater ($\alpha = 0.01$) fine, small, and medium RLD than the herbaceous sites. Because the soil cores were taken 30 cm from the top edge of the bank, these results are only applicable to steep banks with little herbaceous vegetation on the bank face.

Despite this limitation, the results of the root study have significant implications for the use of vegetation in stream bank stabilization. Research by Kamyab (1991) indicated soil erosion was strongly influenced by the quantity of fine roots present. While the herbaceous buffers in this study had a much greater total RLD than the forested buffers, the roots were largely composed of very fine roots that provide less reinforcement against stream bank erosion than the larger diameter roots. Thus, for nearly vertical banks (those without significant vegetation growth on the bank face), woody vegetation may provide better protection against soil scour, especially at the bank toe. This finding is particularly applicable for meandering streams where the region of highest shear stress, the outside of meander bends, is typically very steep and has little herbaceous vegetation on the bank face.

Further study on the effects of root density on stream bank erodibility is necessary. Given the large variability in root density found in this and other studies, future studies should include a large number of root samples taken at the bank face. Results based on a few samples or limited areas may be misleading and may not be applicable beyond the localized environment (McGinty, 1976). The results of this study also illustrate the differences resulting from measurements based on root length versus root volume or root area. Comparing Figures 3.2 and 3.3, it is evident that root volume measurements are biased by larger roots. For studies where the

density of roots in the soil is important, RLD will more accurately represent the overall fiber content than RVR.

Results of this study also showed that stream banks with herbaceous vegetation had higher STs overall and summer diurnal temperature ranges as much as 67% greater than forested stream banks. These differences decreased during the growing season as the herbaceous vegetation matured. Additionally, increases in daily average SWP of 13% to 57% were observed under herbaceous vegetation, as compared to woody vegetation, likely due to evapotranspiration from the shallow herbaceous root system on the bank face. In contrast to summer conditions, the deciduous forest buffers provided little protection for stream banks during the winter: the forested stream banks experienced diurnal temperature ranges two to three times greater than stream banks under dense herbaceous cover and underwent as many as eight times the number of freeze-thaw cycles. With the absence of a dense canopy, the stream banks under mature forest cover were exposed to solar heating and night time cooling, which increased the winter diurnal soil temperature range and the occurrence of freeze-thaw cycling.

In situ jet testing during the summer of 2003 showed the stream bank soils in this study ranged from moderately resistant to very erodible: average $K_d$ and $\tau_c$ values ranged from 0.18 – 13.1 $cm^3$/N-s and from 0.0 – 21.9 Pa, respectively. Several highly significant regression relationships were developed that explained 39 – 99% of the variance in the erosion parameters. Results of this study indicated that soil bulk density is the most significant parameter for determining both the erodibility and critical shear stress of stream bank soils: changes in bulk density alone explained 33 – 52% of the variance in $K_d$ and 36 – 46% of the variance in $\tau_c$. Increases in bulk density resulted in decreases in soil erodibility and increases in the critical shear stress.

Interactions between stream and soil chemical properties also played an important role in soil erodibility and critical shear stress. Increases in the concentrations of the major soil cations reduced $K_d$ while increases in soil pH reduced soil $\tau_c$. The significance of soil chemistry in the susceptibility of stream bank soils to fluvial entrainment depended on the amount and type of clay present.

This research provided quantitative evidence that roots from riparian plants provided significant soil reinforcement. Study results indicated erosion resistance increased with

increasing density of roots with diameters over 0.5 mm. As reported in Chapter 3, the quantity of larger diameter roots is strongly correlated to the quantity of woody vegetation in the riparian buffer. These findings confirmed that woody vegetation provided better reinforcement of stream bank soils due a greater quantity of larger diameter roots. While the effects of roots on stream bank erosion were significant, the analysis also indicated that soil physical and chemical properties played a greater role in soil stability than root reinforcement.

Soil freezing over the previous winter had significant effects on both $K_d$ and $\tau_c$ that varied with soil type. Increases in freeze-thaw cycling (FTC) resulted in increases in soil erodibility for the fine grained, nonreactive soils and decreases in the critical shear stress for nonplastic soils, respectively. In contrast, FTC increased soil stability for fine grained, reactive soils. This contradiction was likely the result of differences in soil structure: the reactive soils were distinct in that they had significantly higher plasticity index values, clay activities, electrical conductivities, and sodium contents. These higher values indicated the more reactive soils had a greater montmorillonite content. As these soils froze, water was removed from the interlayer regions of the clays. This caused the interlayer regions to collapse, increasing soil structure (McBride, 1994). By comparison, the less reactive, fine grained soils had a high silt content and were more susceptible to degradation by ice segregation within the soil. The effects of soil freezing persisted into the summer when testing was conducted, indicating that the effects of FTC were not completely reversed by soil consolidation over time. More information is needed on temporal changes in both $\tau_c$ and $K_d$.

## 6.2. Conclusions

In general, woody riparian vegetation reduced the susceptibility of stream bank soils to erosion by fluvial entrainment. The riparian forests had a greater density of larger diameter roots than the herbaceous buffers, particularly at the bank toe where the hydraulic stresses were the greatest. It was these larger roots (diameters > 0.5 mm) that provided the most resistance to stream bank erosion. Due to limitations in the root sampling methodology, these results are primarily applicable to steep banks with little herbaceous vegetation on the bank face, such as those found on the outside of meander bends. In addition to reinforcing the stream banks, riparian vegetation also affected soil moisture and altered the local microclimate. While the deciduous riparian forests reduced soil desiccation during the summer, they increased freeze-

thaw cycling in the winter. As a result, in silty soils that were susceptible to freeze-thaw cycling, the beneficial effects of root reinforcement by woody vegetation were offset by increased freeze-thaw cycling. Using the study results in an example application, it was shown that converting a predominately herbaceous riparian buffer to a forested buffer could reduce soil erodibility by as much as 39% soils with low silt contents. Conversely, for a stream composed primarily of silt soils that are prone to freeze-thaw cycling, afforestation could lead to localized increases in soil erodibility of as much as 38%. It should be emphasized that the riparian forests in this study were deciduous; similar results would not be expected under coniferous forests that maintain a dense canopy throughout the year. Additionally, because dense herbaceous vegetation would likely not develop in the outside of meander bends where the shear stresses are greatest, the reductions in soil erodibility afforded by the herbaceous vegetation would be limited to areas of low shear stress, such as on gently sloping banks along the inside of meander bends. It should also be noted that this evaluation did not consider the hydraulic effects of woody vegetation (namely reductions in near bank shear stress due to increased roughness with woody vegetation).

Findings from this study suggested that freeze-thaw cycling significantly increased soil erodibility and decreased the critical shear stress. These effects endured over several months and appeared to affect soil within the stream bank, not just on the surface. These results supported Lawler's (1992) premise that freeze-thaw cycling decreases with increasing stream order and the suggestion by Couper and Maddock (2001) that the contribution of subaerial processes (SAP) to stream bank retreat may be underestimated. While mass failure is a dramatic process, producing large amounts of sediment, it is limited temporally and spatially. In contrast, SAP are small in magnitude, but produce frequent erosion over a widespread area. Considering the majority of stream miles in a river system are low order, headwater streams, the effect of SAP on watershed sediment yield may be greater than previously considered. Ultimately, the cumulative impact of SAP at the watershed scale should be investigated, particularly for sediment TMDL planning. Additionally, further study on the effects of SAP on the magnitude of soil erodibility over time is needed to improve estimations of soil loss due to stream bank erosion.

This study provided the first in situ measurements of the soil erosion parameters, $K_d$ and $\tau_c$, for vegetated stream banks. These parameters are crucial for modeling the effects of riparian vegetation for stream restoration design and water quality simulation modeling. The in situ

testing of the erodibility of vegetated stream banks provided a quantitative analysis of the effects of vegetation on stream bank erosion, relative to other soil physical and chemical parameters. Study results indicated that although soil erosion is a complex phenomenon, soil bulk density was a reliable predictor of $K_d$ and $\tau_c$.

While this research provided preliminary data on the effects of vegetation on stream bank soil erodibility, it did not consider all the effects of riparian vegetation on stream morphology. There is a serious lack of information on the impacts of riparian vegetation on near bank shear stresses. The roots of mature trees often extend from the stream banks, providing a rough surface that deflects high velocity flows away from the stream banks. The impact of this roughness needs to be quantified to determine the full impact of riparian vegetation on stream bank erosion.

## 6.3. Research Contributions

This research represents the first quantitative evaluation of the role of vegetation in stream bank erosion. This study provided the first long term continuous record of stream bank soil temperature and moisture and allowed quantification of the cumulative impacts of vegetation on subaerial processes. When combined with the first in situ testing of soil erodibility for vegetated stream banks, these data showed that subaerial processes significantly affected stream bank erodibility. Lastly, by comparing woody and herbaceous vegetation directly, this research showed the effects of vegetation type on stream bank erosion and provided preliminary guidance to watershed managers on selection of vegetation for riparian buffers.

# References Cited


Abernethy, B. and I. D. Rutherfurd. 1998. Where along a river's length will vegetation most effectively stabilize stream banks? *Geomorphology*. 23(1):55-75.

Abernethy, B.I. and D. Rutherfurd. 2000. The effect of riparian tree roots on the mass-stability of riverbanks. *Earth Surface Processes and Landforms*. 25(9):921-937.

Abernethy, B. and I. D. Rutherfurd. 2001. The distribution and strength of riparian tree roots in relation to riverbank reinforcement. *Hydrological Processes*. 15(1):63-79.

Ackers, P. 1992. 1992 Gerald Lacey memorial lecture - Canal and river regime in theory and practice: 1929-1992. *Proc., Inst. Civ. Engrs. Wat., Marit. and Energy*. London, UK. pp. 167-178.

Alizadeh, A. 1974. *Amount and Type of Clay and Pore Fluid Influences on the Critical Shear Stress and Swelling of Cohesive Soils*. PhD Dissertation. University of California at Davis.

Allen, P. M., J. Arnold, E. Jakubowski. 1999. Prediction of stream channel erosion potential. *Environmental & Engineering Geoscience*. V(3):339-351.

Allison, L. E. 1965. Organic carbon. In: C. A. Black, ed. *Methods of Soil Analysis*. American Society of Agronomy: Madison, WI. 1367-1378.

Amarasinghe, I. 1992. *Effects of Root Reinforcement on Soil Strength and Bank Stability*. PhD Thesis. Open University: Milton Keynes, UK.

Anderson, A. G. 1975. Erosion of Sediment – Local Scour. In: Vanoni, V. A. *Sedimentation Engineering*. ASCE Manuals and Reports on Engineering Practice, No. 54. 44-65.

Anderson, M. G., M. G. Hubbard, and P. E. Kneale. 1982. The influence of shrinkage cracks on pore-water pressures within a clay embankment. *Q. Journal of Engineering Geology.* 15(1): 9-14.

Ariathurai, R. and K. Arulanandan. 1978. Erosion rates of cohesive soils. *Journal of the Hydraulics Division*, ASCE. 104 (HY2): 279-283.

ARS. 2003. Helping States Slow Sediment Movement: A High-Tech Approach to Clean Water Act Sediment Requirements. *Agricultural Research Magazine*. 51(12): 12-14.

Arulanandan, K., P. Loganathan, and R. B. Krone. 1975. Pore and eroding fluid influences on surface erosion of soil. *Journal of the Geotechnical Engineering Division, ASCE*. GT1: 51-66.

Arulanandan, K., E. Gillogley, and R. Tully. 1980. *Development of a quantitative method to predict critical shear stress and rate of erosion of natural undisturbed cohesive soils.* Report GL-80-5. USACE Waterways Experiment Station: Vicksburg, MS.

Asare, S. N., R. P. Rudra, W. T. Dickinson, and G. J. Wall. 1997. Frequency of freeze-thaw cycles, bulk density, and saturation effects on soil surface shear and aggregate stability in resisting water erosion. *Canadian Agricultural Engineering*. 39(4): 273-279.

ASCE. 1998a. River width adjustment. I: Processes and mechanisms. *Journal of Hydraulic Engineering*. 124(9):881-902.

ASCE. 1998b. River width adjustment. II: Modeling. *Journal of Hydraulic Engineering*. 124(9):903-917.

ASTM. 1999a. Standard Test Method for Erodibility Determination of Soil in the Field or in the Laboratory by the Jet Index Method, No. D5852-95. ASTM: West Conshohocken, PA. 04.08:686-690.

ASTM. 1999b. Standard Test Methods for Liquid Limit, Plastic Limit, and Plasticity Index of Soils, No. D4318-98. ASTM: West Conshohocken, PA. 4.08:526-538.

ASTM. 1999c. Standard Test Methods for Specific Gravity of Soil Solids by Water Pycnometer, No. D854-92. ASTM: West Conshohocken, PA. 4.08:89-92.

Atkinson, H. B. and C. E. Bay. 1940. Some factors affecting frost-penetration. Transactions, American Geophysical Union, Reports and Papers, Snow Conference, Seattle.

Beeson, C. E. and P. F. Doyle. 1995. Comparison of bank erosion at vegetated and non-vegetated channel bends. *Water Resources Bulletin*. 31(6): 983-990.

Beschta, R.L. and W.S. Platts. 1986. Morphological features of small streams: Significance and function. *Water Resources Bulletin*. 22(3):369-380.

Bicknell, B. R., J. C. Imhoff, J. L. Kittle, Jr., A. S. Donigian, Jr., and Robert C. Johanson. 1997. *Hydrological Simulation Program – Fortran, User's Manual for Version 11*. EPA/600/R-97/080. Environmental Protection Agency: Washington, DC.

Blaisdell, F. W., L. A. Clayton, and G. G. Hebaus. 1981. Ultimate dimensions of local scour. *Journal of the Hydraulics Division, ASCE*. 107(HY3): 327-337.

Böhm, W. 1979. *Methods of Studying Root Systems*. Springer-Verlag: New York.

Bonham, C. D. 1989. *Measurements for Terrestrial Vegetation.* John Wiley & Sons: New York.

Brady, N. C. 1984. *The Nature and Property of Soils*. MacMillan Publishing Co.: New York.

Branson, J., D. M. Lawler, and J. W. Glen. 1996. Sediment inclusion events during needle ice growth: A laboratory investigation of the role of soil moisture and temperature fluctuations. *Water Resources Research*. 32(2): 459-466.

Brown, L. C., G. R. Foster, and D. B. Beasley. 1989. Rill erosion as affected by incorporated crop residue and seasonal consolidation. *Transactions of the ASAE*. 32(6): 1967-1977.

Brown, L. C., L. T. West, D. B. Beasley, and G. R. Foster. 1990. Rill erosion one year after incorporation of crop residue. *Transactions of the ASAE*. 33(5): 1531-1540.

Burn, D. A. and T.A. Ryan, Jr. 1983. A Diagnostic Test for Lack of Fit in Regression Models. *ASA 1983 Proceedings of the Statistical Computing Section.* 286–290.

Carlson, E. J. and P. F. Enger. 1963. *Tractive Force Studies of Cohesive Soils for Design of Earth Canals. Hydraulic Research Report No. HYD-504*. Bureau of Reclamation: Denver, CO.

Chamberlain, E. J. 1981. *Frost Susceptibility of Soil, Review of Index Tests.* Monograph 81-2. U.S. Army cold Regions Research and Engineering Laboratory: Hanover, NH.

Chow, V. T. *Open-Channel Hydraulics*. McGraw-Hill Civil Engineering Series: New York.

Clifton, C. 1989. Effects of vegetation and land use on channel morphology. In: Gresswell, R. E., B. A. Barton, and J. L. Kershner, eds. *Practical Approaches to Riparian Resource Management: An Educational Workshop, May 8-11, 1989, Billings, Montana*. USDI/BLM: Billings, MT. pp. 121-129.

Coppin, N. J. and I. G. Richards. 1990. *Use of Vegetation in Civil Engineering*. Butterworths: London.

Correll, D. L. 1996. Buffer zones and water quality protection: general principles. In: Heycock, N., ed. *Proceedings of the International Conference on Buffer Zones*. Oxford, England, 8/28-9/2, 1996.

Couper, P. 2003. Effects of silt-clay content on the susceptibility of river banks to subaerial erosion. Geomorphology. 56: 95-108.

Craig, R. F. 1992. *Soil Mechanics*. Chapman and Hall: London, UK.

Crépin, J. and R. L. Johnson. 1993. Soil sampling for environmental assessment. In: Carter, M. R. (Ed.). Soil Sampling and Methods of Analysis. Lewis Publishers: Chelsea, MI. 5-18.

Daniel, W. W. 1990. *Applied Nonparametric Statistics*. Boston: PWS-Kent. pp. 306-316.

Daniels, R. B. and J. W. Gilliam. 1996. Sediment and chemical load reduction by grass and riparian filters. *Soil Science Society of America Journal*. 60:246-251.

Davidson, D. W., L. A. Kapustka, and R. G. Koch. 1991. The role of plant root distribution and strength in moderating erosion of red clay in the Lake Superior watershed. *Transactions of the Wisconsin Academy of Sciences, Arts, and Letters*. 77:51-63.

Davies-Colley, R. J. 1997. Stream channels are narrower in pasture than in forest. New Zealand *Journal of Marine and Freshwater Research*. 31:599-608.

Davies-Colley, R. 2000. Can riparian forest be restored without destabilizing stream channels and discrediting managers?. In: Wigington, P. J. and R. L. Beschta, eds. *Riparian Ecology and Management in Multi-Land Use Watersheds, Proceedings, AWRA 2000 Summer Specialty Conference, August 28-31, Portland, OR*. AWRA: Middleburg, VA. pp. 381-385.

Dillaha, T. A., J. H. Sherrard, and D. Lee. 1989. Long-term effectiveness and maintenance of vegetative filter strips. *Water Environment and Technology*. 1(3):418-421.

Dixon, W. J. and A. M. Mood. 1946. The statistical sign test. *Journal of the American Statistical Association.* 41:557-566.

Dunaway, D., S. R. Swanson, J. Wendel, and W. Clary. 1994. The effect of herbaceous plant communities and soil textures on particle erosion of alluvial streambanks. *Geomorphology*. 9:47-56.

Dunn, I. S. 1959. Tractive resistance of cohesive channels. *Proceedings of the Journal of the Soil Mechanics and Foundation Division, ASCE*. 85(SM3):1-24.

Edwards, L. M. and J. R. Burney. 1989. The effect of antecedent freeze-thaw frequency on runoff and soil loss from frozen soil with and without subsoil compaction and ground cover. *Canadian Journal of Soil Science*. 69: 799-811.

Eigenbrod, K. D. 2003. Self-healing in fractured fine-grained soils. *Canadian Geotechnical Journal*. 40: 435-449.

Elliot, W. J., L. J. Olivieri, J. M. Laflen, and K. D. Kohl. 1990. Predicting soil erodibility from soil properties including classification, mineralogy, climate, and topography. ASAE Paper No. 90-2557.

Elzinga, C. L., D. W. Salzer, and J. W. Willoughby. 1998. *Measuring and Monitoring Plant Populations.* BLM Technical Reference 1730-1. US Department of the Interior, Bureau of Land Management: Denver, CO.

FISRWG (Federal Interagency Stream Restoration Working Group). 1998. Stream Corridor Restoration: Principles, Processes, and Practices. NTIS: Washington, DC.

Foster, G. R. 1982. Modeling the erosion process. In: Haan, C. T., H. P. Johnson, and D. L. Brakensiek, eds. *Hydrologic Modeling of Small Watersheds*. ASAE Monograph No. 5. ASAE: St. Joseph, MI. 297-380.

Gray, D. H. and A. T. Leiser. 1982. *Biotechnical Slope Protection and Erosion Control*. Van Nostrand Reinhold, Co.: New York.

Gray, D. H. and A. MacDonald. 1989. The role of vegetation in river bank erosion. In: Ports, M. A., ed. *Hydraulic Engineering, Proceedings of the ASCE Conference*. ASCE: New York. pp. 218-223.

Gray, D. H. and R. B. Sortir. 1996. *Biotechnical and Soil Bioengineering Slope Stabilization: A Practical Guide for Erosion Control*. John Wiley & Sons, Ltd.: New York.

Greene, T. R., S. G. Beavis, C. R. Dietrich, and A. J. Jakeman. 1999. Relating stream-bank erosion to in-stream transport of suspended sediment. *Hydrological Processes*. 13:777-787.

Greenway, D. R. 1987. Vegetation and slope stability. Anderson, M. G. and K. S. Richards, eds. *Slope Stability*. John Wiley & Sons: New York. 187-230.

Gregory, K. J., A. M. Gurnell. 1988. Vegetation and river channel form and process. Viles, H., ed. *Biogeomorphology*. Basil Blackwell: Oxford. pp. 11-42.

Grissinger, E. H. and L. E. Asmussen. 1963. Discussion of Channel stability in undisturbed cohesive soils by E. M. Flaxman. *Journal of the Hydraulics Division*, ASCE. 89(HY6): 259-264.

Grissinger, E. H. 1982. Bank erosion of cohesive materials. In: Hey, R. D., J. C. Bathurst, and C. R. Thorne, eds. *Gravel-bed Rivers*. John Wiley & Sons, Ltd.: New York. pp. 273-287.

Grissinger, E. H., A. J. Bowie, and J. B. Murphey. 1981a. Goodwin Creek bank instability and sediment yield. Proceedings of the Fifth Federal Interagency Sedimentation Conference. PS32-PS39.

Grissinger, E. H., W. C. Little, and J. B. Murphey. 1981b. Erodibility of streambank materials of low cohesion. Transactions of the ASAE. 24(3): 624-630.

Gurnell, A. M. and K. J. Gregory. 1984. The influence of vegetation on stream channel processes. In: Burt, T. P. and D. E. Walling, eds. *Catchment Experiments in Fluvial Geomorphology. Proc. IGU Commission Meeting, Exeter and Huddersfield, UK. Aug. 16-24, 1981*. GeoBooks: Norwich, CT. pp. 515-535.

Hanson, G. J. 1989. Channel erosion study of two compacted soils. Transactions of the ASAE. 32(2):485-490.

Hanson, G. J. 1990a. Surface erodibility of earthen channels at high stresses. Part I - Open channel testing. *Transactions of the ASAE*. 33(1):127-131.

Hanson, G. J. 1990b. Surface erodibility of earthen channels at high stresses. Part II - Developing an in situ testing device. *Transactions of the ASAE*. 33(1):132-137.

Hanson, G. J. 1991. Development of a jet index to characterize erosion resistance of soils in earthen spillways. *Transactions of the ASAE*. 34(5):2015-2020.

Hanson, G. J. and K. R. Cook. 1997. Development of excess shear stress parameters for circular jet testing. ASAE Paper No. 97-2227.

Hanson, G. J. and K. R. Cook. 1998. Relationship of soil suction and erodibility of a compacted soil. ASAE Paper No. 98-2065.

Hanson, G. J. and A. Simon. 2001. Erodibility of cohesive streambeds in the loess area of the midwestern USA. *Hydrological Processes*. 15:23-38.

Hanson, G. J., K. R. Cook, and A. Simon. 1999. Determining erosion resistance of cohesive materials. *Proceedings of the ASCE International Water Resources Engineering Conference, August 8-12, 1999, Seattle, WA.*

Hanson, G. J. 2001. Personal communication on 7/13/2001.

Haynes, R. J. and M. H. Beare. Influence of six crop species on aggregate stability and some labile organic matter fractions. *Soil Biology and Biochemistry*. 29(11-12): 1647-1653.

Heede, B. H. and J. N. Rinne. 1990. Hydrodynamic and fluvial morphological processes and implication for fisheries management and research. *North American Journal of Fisheries Management.*. 10(3):249-268.

Heinzen, R. T. 1976. *Erodibility Criteria for Soils*. MS Thesis, University of California, Davis.

Helsel, D. R. and R. M. Hirsch. 1992. *Statistical Methods in Water Resources*. Elsevier: New York.

Henderson, J. E. 1986. Environmental designs for streambank protection projects. *Water Resources Bulletin*. 22(4):549-558.

Hershfield, D. M. 1974. The frequency of freeze-thaw cycles. *Journal of Applied Meteorology*. 13: 348-354.

Hession, W. C. 2001. Riparian forest and urban hydrology influences on stream channel morphology: Implications for restoration. In: D. Phelps and G. Sehlke, (eds).

*Proceedings of the World Water and Environmental Resources Congress, May 20-24, 2001, Orlando, FL.* ASCE: Reston, VA.

Hettmansperger, T. P. and S. J. Sheather. 1986. Confidence intervals based on interpolated order statistics. *Statistics and Probability Letters*. 4:75-79.

Hey, R. D., C. R. Thorne. 1986. Stable channels with mobile gravel beds. *Journal of Hydraulic Engineering.* 112(8):671-689.

Hickin, E.J. 1984. Vegetation and river channel dynamics. *Canadian Geographer*. 28(2):111-126.

Hodges, Jr., J. L. and E. L Lehmann. 1963. Estimates of location based on rank tests. *Annals of Mathematical Statistics*. 33:482-497.

Hollander, M., and Wolfe, D. A. 1973. *Nonparametric Statistical Methods*. Wiley and Sons: New York.

Hollick, M. 1976. Towards a routine test for the assessment of the critical tractive forces of cohesive soils. *Transactions of the ASAE*. 19(6): 1076-1081.

Holtz, W. G. 1983. The influence of vegetation on the swelling and shrinking of clays in the United States of America. *Geotechnique.* 33:159-163.

Holtz, R. D. and W. D. Kovacs. 1981. *An Introduction to Geotechnical Engineering*. Prentice Hall: Englewood Cliffs, NJ.

Hooke, J. M. 1979. An analysis of the processes of river bank erosion. *Journal of Hydrology*. 42: 39-62.

Horwitz, R. J., W. C. Hession, and B. S. Sweeney. 2000. Effects of forested and unforested riparian zones on stream fishes. In: Wigington, P. J. and R. L. Beschta, eds. *Riparian Ecology and Management in Multi-Land Use Watersheds, Proceedings, AWRA 2000 Summer Specialty Conference, August 28-31, Portland, OR.*

Hupp, C. R. 1999. Relations among riparian vegetation, channel incision processes and forms, and large woody debris. In: Darby, S. E. and A. Simon, eds. *Incised River Channels: Processes, Forms, Engineering, and Management.* John Wiley & Sons: New York. pp. 219-245.

Jackson, D. A. 1993. Stopping rules in principal components analysis: a comparison of heuristical and statistical approaches. *Ecology*. 74: 2204-2214.

Jackson, M. L. 1958. Organic matter determinations for soils. In: *Soil Chemical Analysis*. Prentice-Hall, Inc.: Englewood Cliffs, NJ. 205-266.

Jackson, R. B., J. Canadell, J. R. Ehleringer, H. A. Mooney, O. E. Sala, and E. D. Schulze. 1986. A global analysis of root distributions for terrestrial biomes. *Oecologia*. 108(3): 389-411.

Jennings, G. D., W. A. Harman, D. R. Clinton, and J. L. Patterson. 1999. Stream restoration design experiences in North Carolina. ASAE Paper No. 99-2022.

Johnson R, and D. Wichern. 1992. Applied Multivariate Statistical Methods. 3rd Edition. Upper Saddle River, New Jersey: Prentice Hall.

Johnson, T. E., W. C. Hession, D. F. Charles, R. J. Horwitz, D. A. Kreeger, B. D. Marshall, J. D. Newbold, J. E. Pizzuto, and D. J. Velinsky. 2001. An interdisciplinary study of the ecological benefits of riparian reforestation in urban watersheds. In: D. Phelps, and G. Sehlke, eds., *Proceedings of the World Water and Environmental Resources Congress, May 20-24, 2001, Orlando, FL*. ASCE: Reston, VA.

Jumikis, A. R. 1962. *Soil Mechanics*. Van Nostrand: Princeton, NJ.

Kamyab, I. 1991. *Streambank Stability Prediction for C6 Stream Type Reconstruction*. PhD Dissertation. University of Nevada: Reno, Nevada.

Kandiah, A. 1974. *Fundamental Aspects of Surface Erosion of Cohesive Soils.* PhD Dissertation. University of California: Davis, California.

Kirby, C., M. D. Newson, and K. Gilman. 1991. *Plynlimon Research: The First Two Decades*. Report No. 109. Institute of Hydrology: Wallingford, UK.

Kirkby, M. J. 1967. Measurement and theory of soil creep. *Journal of Geology*. 75:359-378.

Knighton, A. D. 1973. Riverbank erosion in relation to streamflow conditions, River Bollin-Dean, Cheshire. *The East Midland Geographer*. 5:416-426.

Kohnke, H. and C. H. Werkhoven. 1963. Soil temperature and soil freezing as affected by an organic mulch. *Soil Science Society of America Proceedings*. 27: 13-17.

Lambe, T. W. and R. V. Whitman. *Soil Mechanics.* John Wiley & Sons, Inc.: New York.

Langendoen, E. J. 2000. *CONCEPTS - Conservational Channel Evolution and Pollutant Transport System. Research Report No. 16.* USDA-ARS National Sedimentation Laboratory: Oxford, MS.

Laursen, E. M. 1952. Observations on the Nature of Scour. *Proceedings of Fifth Hydraulic Conference, Bulletin 34*. University of Iowa, Iowa City, IA, June 9-11, 1952. 179-197.

Lavelle, W. and H. O. Mofjeld. 1987. Do critical stresses for incipient motion and erosion really exist? *Journal of Hydraulic Engineering*. 113(9): 370-385.

Lawler, D. M. 1986. River bank erosion and the influence of frost: a statistical examination. *Transactions of the Institute of British Geographers.* 11: 227-242.

Lawler, D. M. 1988. Environmental limits of needle ice: a global survey. Arctic and Alpine Research. 20: 137-159.

Lawler, D. M. 1992. Process dominance in bank erosion systems. In: Carling, P. and G. E. Petts, eds. *Lowland Floodplain Rivers*. Wiley: Chichester. pp. 117-143.

Lawler, D. M. 1993. Needle ice processes and sediment mobilization on river banks: The River Ilston, West Glamorgan, UK. *Journal of Hydrology*. 150: 81-114.

Lawler, D. M. 1995. The impact of scale on the processes of channel-side sediment supply: a conceptual model. *Effects of Scale on Interpretation and Management of Sediment and Water Quality*. IAHS Pub. 226. pp. 175-184.

Lawler, D. M., C. R. Thorne, and J. M. Hooke. 1997. Bank erosion and instability., Thorne, C. R. , R. D. Hey, and M. D. Newson, eds. *Applied Fluvial Geomorphology for River Engineering and Management*. John Wiley & Sons: Chichester. 138-172

Lawler, D. M., J. R. Grove, J. S. Couperthwaite, G. J. L. Leeks. 1999. Downstream change in river bank erosion rates in the Swale-Ouse system, northern England. *Hydrological Processes*. 13(7): 977-992.

Laursen, E. 1958. The total sediment load of streams. *Journal of the Hydraulics Division.* 84(HY1). 1530-1 - 1530-36.

Le Bissonnais, Y. 1996. Aggregate stability and assessment of soil crustability and erodibility: I. Theory and methodology. *European Journal of Soil Science*. 47: 425-437.

Lehrsch, G. A., R. E. Sojka, D. L. Carter, and P. M. Jolley. 1991. Freezing effects on aggregate stability affected by texture, mineralogy, and organic matter. *Soil Science Society of America Journal.* 55: 1401-1406.

Lehrsch, G. A. 1998. Freeze-thaw cycles increase near-surface aggregate stability. *Soil Science.* 163(1): 63-70.

Leopold, L. B. and T. Maddock, Jr. 1953. The hydraulic geometry of stream channels and some physiographic implications. Professional Paper 252. USGS: Reston, VA.

Leopold, L. B., M. G. Wolman, and J. P. Miller. 1964. *Fluvial Processes in Geomorphology.* Freeman: San Francisco, CA.

Lowrance, R., L. S. Altier, J. D. Newbold, R. R. Schnabel, P.M. Groffman, J. M. Denver, D. L. Correll, J. W. Gilliam, J. L. Robinson, R. B. Brinsfield, K. W. Staver, W. Lucas, and A. H. Todd. 1995. *Water Quality Functions of Riparian Forest Buffer Systems in the Chesapeake Bay Watershed*. EPA 903-R-95-004. USEPA: Washington, DC.

Lyle, W. M. and E. T. Smerdon. 1965. Relation of compaction and other soil properties to the erosion resistance of soils. *Transactions of the ASAE*. 8(3):419-422.

Lyons, J., S. W. Trimble, and L. K. Paine. 2000. Grass versus trees: Managing riparian areas to benefit streams of central North America. *Water Resources Bulletin.* 36(4):919-930.

Mackin, J. H. 1948. Concept of the graded river. *Geological Society of America Bulletin.* 59:463-512.

Mamo, M. and G. D. Bubenzer. 2001a. Detachment rate, soil erodibility, and soil strength as influenced by living plant roots, Part I: Laboratory Study. Transactions of the ASAE. 44(5): 1167-1174.

Mamo, M. and G. D. Bubenzer. 2001b. Detachment rate, soil erodibility, and soil strength as influenced by living plant roots, Part I: Field Study. Transactions of the ASAE. 44(5): 1175-1181.

Martin, T. R. 1962. Discussion of Experiments on the sour resistance of cohesive sediments. *Journal of Geophysical Research*. 67(4): 1447-1449.

Masterman, R, and C. R. Thorne. 1992. Predicting influence of bank vegetation on channel capacity. *Journal of Hydraulic Engineering*. 118(7): 1052-1058.

Materechera, S. A., A. R. Dexter, and A. M. Alston. 1992. Formation of aggregates by plant roots in homogenized soils. *Plant and Soil*. 142: 69-79.

Matsuoka, N. 1996. Soil moisture variability in relation to diurnal frost heaving on Japanese high mountain slopes. *Permafrost and Periglacial Processes*. 7: 139-151.

McBride, M. B. 1994. *Environmental Chemistry of Soils*. Oxford University Press: New York.

McKenney, R., R. B. Jacobson, and R. C. Wertheimer. 1995. Woody vegetation and channel morphogenesis in low gradient, gravel bed streams in the Ozark Plateaus, Missouri and Arkansas. *Geomorphology*. 13(1-4):175-198.

Micheli, E. R. and J. W. Kirchner. 2002. Effects of wet meadow riparian vegetation on streambank erosion. 2. Measurements of vegetated bank strength and consequences for failure mechanics. *Earth Surface Processes and Landforms*. 27(7): 687-697.

Montgomery, D. C. and E. A. Peck. 1982. *Introduction to Linear Regression Analysis*. John Wiley & Sons: New York.

Moore, W. L. and F. D. Masch. 1962. Experiments of the scour resistance of cohesive sediments. *Journal of Geophysical Research*. 67(4): 1437-1446.

Mosley, M. P. 1981. Semi-determinate hydraulic geometry of river channels, South Island, New Zealand. *Earth Surface Processes and Landforms*. 6:127-137.

Mostaghimi, S., R. A. Young, A. R. Wilts, and A. L. Kenimer. 1988. Effects of frost action on soil aggregate stability. *Transactions of the ASAE*. 31:435-439.

Murgatroyd, A. L. and J. L. Ternan. 1983. The impact of afforestation on stream bank erosion and channel form. *Earth Surface Processes and Landforms*. 8(4):357-370.

Nearing, M. A., L. T. West, and L. C. Brown. 1988. A consolidation model for estimating changes in rill erodibility. *Transactions of the ASAE.* 31(3): 696-700.

Neave, H. R. and P. L. Worthington. 1988. *Distribution-Free Tests*. Unwin Hyman: London.

O'Laughlin, J. 1995. Functional approaches to riparian buffer strip design. *Journal of Forestry*. 93(2):29-32.

Odgaard, A. J. 1987. Streambank erosion along 2 rivers in Iowa. *Water Resources Research*. 23(7): 1225-1236.

Osman, A. M. and C. R. Thorne. 1988. Riverbank stability analysis I: Theory. *Journal of Hydraulic Engineering*. 114:134-150.

Ott, R. L. 1993. *An Introduction to Statistical Methods and Data Analysis*. Duxbury Press: Belmont, CA.

Outcalt, S. I. 1971. An algorithm for needle ice growth. *Water Resources Research*. 7(2):394-400.

Owoputi, L. O. and W. J. Stolte. 1995. Soil detachment in the physically based soil erosion process: A review. *Transactions of the ASAE*. 38(4): 1099-1110.

Oztas, T. and F. Fayetorbay. 2003. Effect of freezing and thawing processes on soil aggregate stability. *Catena*. 52(1): 1-8.

Paaswell, R. E. 1973. Causes and mechanisms of cohesive soil erosion: The state of the art. In: *Soil Erosion: Causes and Mechanisms: Prevention and Control,* Special Report No. 135. Highway Research Board, National Academy of Science: Washington, DC. 52-74.

Palone, R. S. and A. H. Todd (eds.). 1997. *Chesapeake Bay Riparian Handbook: A Guide for Establishing and Maintaining Riparian Forest Buffers.* USDA Forest Service. NA-TP-02-97. Radnor, PA.

Peach, M. 1965. Hydrogen ion activity. In: Black, C. A. (ed.). *Methods of Soil Analysis, Part 2, Chemical and Microbiological Propertie*s. Agronomy No. 9. American Society of Agronomy Inc.: Madison, Wisconsin. 914-926.

Pikul, J. L., Jr. and R. R. Allmaras. 1985. Hydraulic potential in unfrozen soil in response to diurnal freezing and thawing of the soil surface. *Transactions of the ASAE*. 28:164-168.

Pizzuto, J. E. and T. S. Meckelnburg. 1989. Evaluation of a linear bank erosion equation. *Water Resources Research*. 25(5):1005-1013.

Prosser, I.P., A. O. Hughes, and I. D. Rutherfurd. 2000. Bank erosion of an incised upland channel by subaerial processes: Tasmania, Australia. *Earth Surface Processes and Landforms*. 25(10):1085-1101.

Reed, J. M. 1999. *A Comparison of Bed Material Transport Through Forested and Grassed Reaches of a Small Gravel Bedded Stream of the PA Piedmont.* MS Thesis - University of Delaware.

Reid, J. B. and M. J. Goss. 1981. Effect of living roots of different plant species on the aggregate stability of two soils. *Journal of Soil Science*. 32: 521-54.

Reid, J. B. and M. J. Goss. 1980. Changes in aggregate stability of a sandy loam effected by growing roots of perennial ryegrass (Lolium perenne). *Journal of the Science of Food and Agriculture*. 31: 325-328.

Rinaldi, M. and N. Casagli. 1999. Stability of streambanks formed in partially saturated soils and effects of negative pore water pressures: the Sieve River (Italy). *Geomorphology.* 26(4): 253-277.

Roberts, J., R. Jepsen, D. Gotthard, and W. Lick. 1998. Effects of particle size and bulk density on erosion of quartz particles. *Journal of Hydraulic Engineering*. 124 (12): 1261-1267.

Robinson, K. M., S. J. Bennett, and G. J. Hanson. 2000. The influence of weathering on headcut erosion. ASAE Paper No. 00-2066.

Roseboom, D., K. Russell. 1985. Riparian vegetation reduces stream bank and row crop flood damages. *Riparian Ecosystems and Their Management: Reconciling Conflicting Uses, First North American Riparian Conference, April 16-18, 1985, Tucson, AZ,* General Technical Report RM-120. USDA Forest Service. 241-244.

Rosgen, D. 1996. *Applied River Morphology*. Wildland Hydrology: Pagosa Springs, CO.

Rouse, H. 1940. Criteria for similarity in the transportation of sediment. *Proceedings of the First Hydraulic Conference, Bulletin 2*0, State University of Iowa, Iowa City, IA, March 1940. 33-49.

Schumm, S. A. and R. W. Lichty. 1965. Time, space and causality, in geomorphology. *American Journal of Science*. 263:110-119.

Shaw, P. J. A. 2003. *Multivariate Statistics for the Environmental Sciences.* Arnold: London.

Shiel, R. S., M. A. Adey, and M. Lodder. The effect of successive wet/dry cycles on aggregate size distribution in a clay texture soil. *Journal of Soil Science*. 39:71-80.

Shields, Jr., F. D. and D. H. Gray. 1992. Effects of woody vegetation on sandy levee integrity. *Water Research Bulletin*. 28(5):917-931.

Shields Jr., F. D., A. J. Bowie, and C. M. Cooper. 1995. Control of streambank erosion due to bed degradation with vegetation and structure. *Water Resources Bulletin*. 31(3):475-489.

Simon, A. and S. Darby. 1999. The nature and significance of incised river channels. In: Darby, S. E. and A. Simon, eds. *Incised River Channels: Processes, Forms, Engineering, and Management.* John Wiley & Sons: New York. pp. 3-18.

Simon, A., A. Curini, S. Darby, and E. J. Langendoen. 1999. Streambank mechanics and the role of bank and near-bank processes in incised channels. In: Darby, S. E. and A. Simon, eds. *Incised River Channels: Processes, Forms, Engineering and Management*. John Wiley & Sons, Ltd.: Chichester. pp. 123-152.

Simon, A., A. Curini, S. E. Darby, and E. J. Langendoen. 2000. Bank and near-bank processes in an incised channel. *Geomorphology*. 35(3-4):193-217.

Simon, A. 2001. Personal communication on 8/14/2001.

Simon, A. and A. Collison. 2001. Scientific basis for streambank stabilization using riparian vegetation. *Proceedings of the 7th Federal Interagency Sedimentation Conference, Reno, NV.* pp. V-47-54.

Simon, A. and A. Collison. 2002. Quantifying the mechanical and hydrologic effects of riparian vegetation on stream bank stability. *Earth Surface Processes and Landforms*. 27:527-546.

Smerdon, E. T. and R. P. Beasley. 1965. The tractive force theory applied to stability of open channels in cohesive soil. *Research Bulletin 715*. Agricultural Experiment Station, University of Missouri: Columbia, MO.

Smith, C. 1992. Riparian afforestation effects on water yields and water quality in pasture catchments. *Journal of Environmental Quality*. 21:237-245.

Stein, O. R., P. Y. Julien, and C. V. Alonso. 1993. Mechanics of jet scour downstream of a headcut. *Journal of Hydraulic Research*. 31(6): 723-738.

Stein, O. R. and D. D. Nett. 1997. Impinging jet calibration of excess shear sediment detachment parameters. *Transactions of the ASAE*. 40(6): 1573-1580.

Stott, T. 1997. A comparison of stream bank erosion processes on forested and moorland streams in the Balquhidder catchments, central Scotland. *Earth Surface Processes and Landforms*. 22(4):383-399.

Stott, T. A., R. I. Ferguson, R. C. Johnson, and M. D. Newson. 1986. Sediment budgets in forested and unforested basins in upland Scotland. In: Hadley, R. F., ed. *Drainage Basin Sediment Delivery: Proceedings of the Albuquerque Symposium.* IAHS Pub. 159. IAHS. pp. 57-68.

Sun, G. W., D. P Coffin, and W. K. Lauenroth. 1997. Comparison of root distributions of species in North American grasslands using GIS. Journal of Vegetation Science. 8(4): 587-596.

Sweeney, B. W. 1992. Streamside forests and the physical, chemical, and trophic characteristics of piedmont streams in eastern North America. *Water Science and Technology*. 26:2653-2673.

Sweeney, B. W. 1993. Effects of streamside vegetation on macroinvertebrate communities of White Clay Creek in eastern North America. *Proceedings of The Academy of Natural Science of Philadelphia*. pp. 291-340.

Tengbeh, G. T. 1993. The effect of grass roots on shear strength variations with moisture content. *Soil Technology*. 6: 287-295.

Thompson, W. R. 1936. On confidence ranges for the median and other expectation distributions for populations of unknown distribution form. *Annals of Mathematical Statistics.* 7:122-128.

Thorne, C. R. and N. K. Tovey. 1981. Stability of composite river banks. *Earth Surface Processes and Landforms*. 6(5):469-484.

Thorne, C. R. 1982. Processes and mechanisms of river bank erosion. In: Hey, R. D., J. C. Bathurst, and C. R. Thorne, eds. *Gravel-bed Rivers*. John Wiley & Sons, Ltd.: New York. pp. 227-259.

Thorne, C. R. and A. M. Osman. 1988. Riverbank stability analysis. II. Applications. J*ournal of Hydraulic Engineering*. 114:151-173.

Thorne, C. R. 1990. Effects of vegetation on riverbank erosion and stability. In: Thornes, J. B., ed. *Vegetation and Erosion: Processes and Environments.* John Wiley & Sons: Chichester, UK. pp. 125-144.

Thorne, C., I. Amarasinghe, J. Gardiner, C. Perala-Gardiner, R. Sellin, M. Greaves, and J. Newman. 1997. *Bank Protection using Vegetation with Special Reference to Willows: Project Record*. Engineering and Physical Science Research Council and Environment Agency: UK.

Thorne, S. D. and D. J. Furbish. 1995. Influences of coarse bank roughness on flow within a sharply curved river bend. *Geomorphology*. 12(3):241-257.

Trimble, S. W. 1997a. Contribution of stream channel erosion to sediment yield from an urbanizing watershed. *Science*. 278:1442-1444.

Trimble, S. W. 1997b. Stream channel erosion and change resulting from riparian forests. *Geology*. 25(5):467-469.

Tsujimoto, T. 1999. Sediment transport processes and channel incision: Mixed size sediment transport, degradation, and armouring. In: Darby, S. E. and A. Simon, eds. *Incised River Channels: Processes, Forms, Engineering, and Management*. John Wiley & Sons: New York. pp. 38-66.

Tufekcioglu, A. and J. W. Raich, T. M. Isenhart, R. C. Schultz. 1999. Fine root dynamics, coarse root biomass, root distribution, and soil respiration in a multispecies riparian buffer in Central Iowa, USA. *Agroforestry Systems*. 44(2/3):163-174.

USACE. 1981. *Final Report to Congress: The Streambank Erosion Control and Evaluation Demonstration Act of 1974. Main Report.* US Army Corps of Engineers: Washington, DC.

USACE. 1993. *HEC-6: Scour and Deposition in Rivers and Reservoirs, User's Manual, Version 4.1*. Department of the Army, US Army Corps of Engineers, Hydrologic Engineering Center: Alexandria, VA.

USACE. 1994. *Channel stability assessment for flood control projects : engineering and design.* EM1110-2-1418. Department of the Army, US Army Corps of Engineers: Washington, DC.

USDA. 1996. *Soil Survey Laboratory Manual Methods. Soil Survey Investigations Report No. 42, Version 3.0*. US Department of Agriculture, Natural Resources Conservation Service, National Soil Survey Center: Lincoln, NE.

USEPA. 1983. Methods for Chemical Analysis of Water and Wastes. US Environmental Protection Agency: Washington, DC.

USEPA. 2002. *National Water Quality Inventory: 2000 Report*. EPA 841-R-02-001. USEPA: Washington, DC.

VADEQ. 2002. *Drought Status Report: September 20, 2002*. Drought Monitoring Task Force, Virginia Department of Environmental Quality: Richmond, VA.

Van Miegroet, H., D. Zabowski, C. T. Smith, and H. Lundkvist. 1984. Review of measurement techniques in site productivity studies. Dyck, W. J., D. W. Cole, and N. B. Comerford (eds.). *Impacts of Forest Harvesting on Long-Term Site Productivity*. Chapman and Hall: New York. 287-362.

Vanoni, V. A. 1975. *Sedimentation Engineering*. ASCE Manuals and Reports on Engineering Practice, No. 54.

VeriTech, Inc. 1999. Streambank Stabilization Handbook, Version 1.0. Veri-Tech, Inc.: Vicksburg, MS. CD-ROM.

Waldron, L. J. and S. Dakessian. 1981. Soil reinforcement by roots: calculation of increased soil shear resistance from root properties. *Soil Science*. 132(6):427-435.

Waldron, L. J. and S. Dakessian. 1982. Effect of grass, legume, and tree roots on soil shearing resistance. *Soil Science Society of America Journal.* 46(5):894-899.

Walkley, A. and I. A. Black. 1934. An examination of the Deggareff method for determining soil organic matter, and a proposed modification of the chromic acid titration method. *Soil Science*. 37: 29-38.

Wang, L., J. Lyons, and P. Kanehl. 2003. Impacts of urban land cover on trout streams in Wisconsin and Minnesota. *Transactions of the American Fisheries Society*. 132: 825-839.

West, L. T., W. P. Miller, R. R. Bruce, G. W. Langdale, J. M. Laflen, and A. W. Thomas. 1992. Cropping system and consolidation effect on rill erosion in Georgia Piedmont. *Soil Science Society of America Journal*. 56: 1238-1243.

Wilcoxon, F. 1945. Individual comparisons by ranking methods. *Biometrics*. 1:80-83.

Wischmeier, W. H. and J. V. Mannering. 1969. Relation of soil properties to its erodibility. *Soil Science Society of America Proceedings.* 33(1): 131-137.

Wolman, M. G. 1955. *The Natural Channel of Brandywine Creek*. Professional Paper 271. USGS: Reston, VA.

Wolman, M. G. 1959. Factors influencing erosion of a cohesive river bank. *American Journal of Science*. 257:204-216.

Wood, A. L. 2001. *A Geomorphological Analysis of Bank Toe Processes: The Fate of Failed Blocks Stored in the Basal Zone of Incised Channels*. PhD Dissertation, University of Nottingham.

Wu, T. H. 1984. Effect of vegetation on slope stability. *Transportation Research Record*. Transportation Research Board, National Research Council: Washington, DC. 965:37-46.

Wu, T. H. and W. P. McKinnell. 1976. Strength of tree roots and landslides on Prince of Wales Island, Alaska. *Canadian Geotechnical Journal*. 16:19-33.

Zein el Abedine, A. and G. H. Robinson. 1971. A study on cracking in some vertisols of the Sudan. *Geoderma*. 5: 229-241.

Zimmerman, R. C., J. C. Goodlett, and G. H. Comer. 1967. The influence of vegetation on channel form of small streams. *Symposium on River Morphology*, Publication No. 75. International Assoc. Sci. Hydrol. pp. 225-275.